

19930093380

L-190

ARR No. L5F01

NATIONAL ADVISORY COMMITTEE FOR AERONAUTICS

WARTIME REPORT

ORIGINALLY ISSUED

June 1945 as
Advance XXXXXXXXXX Report L5F01

COLUMN AND PLATE COMPRESSIVE STRENGTHS

OF AIRCRAFT STRUCTURAL MATERIALS

24S-T ALUMINUM-ALLOY SHEET

By Eugene E. Lundquist, Evan H. Schuette,
George J. Heimerl, and J. Albert Roy

Langley Memorial Aeronautical Laboratory
Langley Field, Va.

PROPERTY OF ENGINEERING LIBRARY
TEMCO AIRCRAFT CORPORATION



WASHINGTON

NACA WARTIME REPORTS are reprints of papers originally issued to provide rapid distribution of advance research results to an authorized group requiring them for the war effort. They were previously held under a security status but are now unclassified. Some of these reports were not technically edited. All have been reproduced without change in order to expedite general distribution.

NATIONAL ADVISORY COMMITTEE FOR AERONAUTICS

ADVANCE ~~PRELIMINARY~~ REPORT

COLUMN AND PLATE COMPRESSIVE STRENGTHS
OF AIRCRAFT STRUCTURAL MATERIALS

24S-T ALUMINUM-ALLOY SHEET

By Eugene E. Lundquist, Evan H. Schuette
George J. Heimerl, and J. Albert Roy

SUMMARY

Column and plate compressive strengths of 24S-T aluminum-alloy sheet were determined both within and beyond the elastic range from tests of thin-strip columns and from local-instability tests of formed Z- and channel-section columns. These tests are the first of a series in an extensive research investigation to provide data on the structural strength of various aircraft materials. The results, which are presented in the form of curves and charts that may be used in the design and analysis of aircraft structures, supersede preliminary results published previously.

INTRODUCTION

Column and plate members in an aircraft structure are the basic elements that fail by instability. If efficient structures are to be designed, the strength of these elements must be known for the various aircraft materials. An extensive research program has therefore been undertaken at the Langley Memorial Aeronautical Laboratory to establish the column and plate compressive strengths for a number of the alloys available for use in aircraft structures. Reliable and rapid procedures for testing such materials have already been developed and are described in references 1 and 2.

The first material tested during the present investigation was 24S-T aluminum-alloy sheet. The results for this material, given herein, supersede those contained in a preliminary report (reference 2).

SYMBOLS

- L length of column
- ρ radius of gyration
- c fixity coefficient used in Euler column formula
- $\frac{L}{\rho\sqrt{c}}$ effective slenderness ratio of thin-strip column
- b width of plate
- b_F width of flange of Z- or channel section (see fig. 1)
- b_W width of web of Z- or channel section (see fig. 1)
- r inside radius of bend of Z- or channel section
(see fig. 1)
- t thickness of plate
- k nondimensional coefficient used in plate-buckling formula
- k_W coefficient k used with b_W and t in plate-buckling formula (see fig. 2 and reference 3)
- E_c modulus of elasticity in compression, taken as 10,700 ksi for 24S-T aluminum alloy
- τ nondimensional coefficient for columns (The value of τ is so determined that when the effective modulus τE_c is substituted for E_c in the equation for elastic buckling of columns, the computed critical stress agrees with the experimentally observed value. The coefficient τ is equal to unity within the elastic range and decreases with increasing stress beyond the elastic range.)
- η nondimensional coefficient for plates corresponding to τ for columns
- μ Poisson's ratio, taken as 0.3 for 24S-T aluminum alloy

σ_{cr} critical compressive stress

$\bar{\sigma}_{max}$ average compressive stress at maximum load

σ_{cy} compressive yield stress

METHODS OF TESTING AND ANALYSIS

All tests were made in hydraulic testing machines accurate to within three-fourths of 1 percent. The ends of the stress-strain specimens and the columns were ground flat and square.

Stress-strain curves.- The compressive stress-strain data, which identify the material for correlation with its column and plate compressive strengths, were obtained from tests of single-thickness specimens in a compression fixture of the Montgomery-Templin type shown in figure 3. This fixture was used only for flat compression specimens, which represented the material before forming. Information on the technique used in making these tests is presented in reference 4. For the bent material in the corners of the formed Z- and channel sections, compression specimens were cut from the corner portion and tested in the special fixture shown in figure 4.

Column strength.- The column strength and the associated effective column modulus were obtained by testing thin-strip columns of the material with the ends clamped in fixtures of the type shown in figure 5. The use of end fixtures of this type is discussed in detail in reference 1. The fixtures used have been improved, and the method of analysis has been modified since the publication of reference 1. The method now used results in a column curve representative of nearly perfect column specimens. In addition, the method now takes into account the fact that columns of the dimensions tested are actually plates with two free edges.

Plate compressive strength.- The plate compressive strength of the material was obtained from compression tests on Z- and channel-section columns so proportioned as to develop local instability, that is, instability of the plate elements of which they are comprised. (See fig. 6.) Inasmuch as the flanges and webs of such columns are in reality plates with various kinds of edge support,

the problem of local instability of these columns is a plate-buckling problem, and the plate compressive strength of the material was evaluated from these tests. The lengths of the columns were so chosen as to avoid column failure and still provide satisfactory local-instability data. These considerations are discussed in reference 5.

The Z- and channel-section columns were tested with the ends bearing directly against the testing-machine heads, which were carefully aligned to insure uniform bearing on the column ends. A Z-section column under test is shown in figure 7. The relative displacements of pointers, which were supported by extension arms attached to the flanges of the specimens, were measured by the optical micrometers that can be seen in figure 7. The displacement was taken as a measure of the cross-sectional distortion, and the critical compressive stress was obtained from stress-distortion curves of the type illustrated in figure 8. The critical stress was determined as the stress at the point near the top of the knee of the stress-distortion curve at which a marked increase in distortion first occurred with small increase in stress. (See fig. 8.)

RESULTS AND DISCUSSION

Because the compressive properties of aluminum-alloy sheet may vary appreciably, the data and charts of the present report should not be applied to the design of structures of 24S-T aluminum-alloy sheet having compressive properties appreciably different from those reported herein unless a suitable method is devised for adjusting test results to account for variations in material properties.

Compressive Stress-Strain Curves

Compressive stress-strain curves obtained for the flat sheet material used in making the columns are given in figure 9 for both directions of grain. The Z-, channel, or thin-strip columns to which a particular stress-strain curve applies are indicated in table 1, together with the value of the compressive yield stress σ_{cy} for that stress-strain curve. These values average approximately 44 ksi for the flat sheet material in the with-grain direction

and 49 ksi in the cross-grain direction. The modulus of elasticity in compression was taken as 10,700 ksi, the accepted value for 24S-T aluminum alloy.

When the flat sheet material is bent to an inside radius r of $3t$ to form a Z or channel, the cold work done on the material evidently raises the compressive yield stress for the curved corner portion above that for the flat web or flange, about 18 percent for the with-grain and 10 percent for the cross-grain direction. (See fig. 10.) Because the curved corner specimens included along their edges some flat material (about 40 percent of the total area) for which the yield stress is lower than that for the curved portion, the actual increase in the compressive yield stress for the corner portion may be somewhat greater than the increase indicated in figure 10. The important result to note is that the compressive properties of a formed section may not be uniform over the cross section.

Column Strength

The results of the tests of the thin-strip columns are given by the column curves of figure 11 for the two directions of grain.

At stresses beyond the elastic range, the experimental values of σ_{cr} are lower than those computed by the Euler column formula (see elastic-buckling curve, fig. 11), because of the reduction in the effective modulus of elasticity. The effective modulus to be substituted for E_c in the Euler column formula to bring calculated and experimental values of σ_{cr} into agreement is given as τE_c , where τ is a coefficient that is equal to unity in the elastic range and decreases with increasing stress beyond the elastic range. In structural calculations in which it is impossible to use directly values obtained from the column curve (fig. 11), the value of τ for a given stress must be known. The variation of τ with stress for columns is therefore shown in figure 12 for both directions of grain.

Plate Compressive Strength

The results of the local-instability tests of the formed Z- and channel-section columns, used to determine the plate compressive strength, are given in tables 2 and 3. The important relationships for compressed plates obtained from these tests are shown on the curves and design charts presented in the following paragraphs.

Plate-buckling curve.— The plate-buckling curve, which is analogous to the column curve, is shown in figure 13 for plates loaded in the with-grain direction. The abscissa in figure 13 is suggested by transposing the plate-buckling equation

$$\sigma_{cr} = \frac{k\pi^2 E_c t^2}{12(1-\mu^2)b^2} \quad (1)$$

to the form

$$\sigma_{cr} = \frac{\pi^2 E_c}{\left[\frac{b_W}{t} \sqrt{\frac{12(1-\mu^2)}{k_W}} \right]^2} \quad (2)$$

where the subscript W is added to make the terms b and k of the equation correspond to the entries in tables 2 and 3. The similarity between the form of equation (2) and the following form of the Euler column formula is to be noted:

$$\sigma_{cr} = \frac{\pi^2 E_c}{\left(\frac{L}{\rho/c} \right)^2} \quad (3)$$

At stresses beyond the elastic range, as in the case of columns, the experimental values of σ_{cr} for plates are lower than those given by equation (2) for elastic buckling (see elastic-buckling curve, fig. 13), because of the reduction in the effective modulus of elasticity. The effective plate modulus corresponding to πE_c for columns is given as πE_c , and the variation of η with

stress is given, together with the variation of τ , in figure 12. The crossing of the τ - and η -curves shown in figure 12 occurs because the formed columns apparently had an appreciable degree of imperfection, which resulted in the deviation of the η -curve from unity at a lower stress than that at which the τ -curve, representative of nearly perfect columns, deviates from unity.

Relationship of σ_{cr} to σ_{cr}/η for plates.- In problems concerned with the strength of plates, it is sometimes desirable to insert the value of ηE_c for E_c in the plate-buckling formula, equation (1), and to write the equation in the transposed form

$$\frac{\sigma_{cr}}{\eta} = \frac{k\pi^2 E_c t^2}{12(1-\mu^2)b^2} \quad (4)$$

In this form the value of σ_{cr}/η is given by the modulus of elasticity, Poisson's ratio, the geometric dimensions of the plate, and the coefficient k . The value of σ_{cr} can then be obtained by use of the curve of σ_{cr} against σ_{cr}/η given in figure 14. This curve may be obtained by plotting the data directly or by plotting from the faired curves of figure 13.

As in the case of equation (1), the subscripts W may be added to k and b of equation (4), and σ_{cr}/η may be determined for a Z- or channel-section by the use of the formula and curve of figure 2.

Maximum compressive strength of plate elements.- In the case of a plate loaded in longitudinal compression, the supported, or restrained and supported, side edges remain essentially straight after buckling and are capable of carrying additional load. As a consequence, there is a maximum strength for the plate that is greater than the buckling strength.

Theoretical studies that appear in the literature concerning the ultimate strength of plates and the associated effective width of the plates after buckling indicate that the average stress at maximum load is related to the critical stress. It is therefore reasonable to assume that the average stress at maximum load

$\bar{\sigma}_{\max}$ for the combination of plate elements that make up the Z- or channel-section column is also related to the critical stress for the combination. Accordingly, the experimental values obtained are plotted in figure 15 as σ_{cr} against the ratio $\sigma_{cr}/\bar{\sigma}_{\max}$, and from this figure a definite relationship is seen to exist between σ_{cr} and $\bar{\sigma}_{\max}$ for a given value of b_w/t .

In some cases, values of $\bar{\sigma}_{\max}$ rather than σ_{cr} may be required in strength calculations. The values of $\bar{\sigma}_{\max}$ are therefore plotted against σ_{cr}/η in figure 16. The feasibility of making such a plot is indicated by the relationship between σ_{cr} and σ_{cr}/η shown in figure 14 and the relationship between $\bar{\sigma}_{\max}$ and σ_{cr} shown in figure 15. Figure 16 is particularly useful because the quantity σ_{cr}/η is determined by known quantities according to the formula and curve of figure 2.

The reason for the difference in the curves of figures 15 and 16 for different values of b_w/t is not fully understood. The stress-strain curves have indicated, however, that the bending of the material in the forming of the columns raises the compressive yield stress for the material in the corners. (See fig. 10.) An examination of the data showed that as b_w/t is reduced for a given thickness t and a given value of σ_{cr}/η , the total cross-sectional area is also reduced; the fixed area of high-strength bent material in the corners therefore becomes a higher percentage of the total area. This fact may account for the higher values of $\bar{\sigma}_{\max}$ obtained at given values of σ_{cr}/η for the Z- and channel-section columns with lower values of b_w/t . (See fig. 16.)

Effect of grain direction on plate strength.- The data on plate strength presented in figures 13 to 16 were obtained from columns loaded in the with-grain direction. In order to determine the effect of grain direction on the values of σ_{cr} and $\bar{\sigma}_{\max}$, a few columns were constructed and tested with the grain of the sheet at right angles to the axis of the column. These columns are herein designated cross-grain columns.

In figures 17 and 18, the data obtained from the cross-grain columns are plotted as experimental points

for comparison with curves taken from figures 14 and 16 for the with-grain columns. Only at the higher stresses, where the stress-strain curve for the cross-grain direction differs noticeably from the stress-strain curve for the with-grain direction, are the values of σ_{cr} and $\bar{\sigma}_{max}$ greater for the cross-grain columns than for the with-grain columns. The average increase in the high-stress region was about 4 percent for σ_{cr} and about 2 percent for $\bar{\sigma}_{max}$; whereas the cross-grain compressive yield stress was approximately 11 percent greater than the with-grain compressive yield stress.

Charts for local instability of Z- and channel-section columns.- The plate compressive strength of the material was evaluated from tests of Z- and channel-section columns. The results of these tests, which provided this information regarding plates, may also be applied directly to formed Z- and channel-section columns that fail by local instability. These results can be conveniently summarized in the form of charts that give directly, in terms of the dimension ratios b_F/b_W and b_W/t , the critical stress and the average stress at maximum load. Such charts, based on the theoretical curve of figure 2 and the experimental data, are given in figures 19 to 21.

CONCLUDING REMARK

The important conclusions of this report are embodied in the test data of column and plate compressive strengths, which are presented in the form of curves and charts that may be used in the design and analysis of aircraft structures of 24S-T aluminum-alloy sheet.

Langley Memorial Aeronautical Laboratory
National Advisory Committee for Aeronautics
Langley Field, Va.

REFERENCES

1. Lundquist, Eugene E., Rossman, Carl A., and Houbolt, John C.: A Method for Determining the Column Curve from Tests of Columns with Equal Restraints against Rotation on the Ends. NACA TN No. 903, 1943.
2. Heimerl, George J., and Roy, J. Albert: Preliminary Report on Tests of 243-T Aluminum-Alloy Columns of Z-, Channel, and H-Section That Develop Local Instability, NACA RB No. 3J27, 1943.
3. Kroll, W. D., Fisher, Gordon P., and Heimerl, George J.: Charts for Calculation of the Critical Stress for Local Instability of Columns with I-, Z-, Channel, and Rectangular-Tube Section. NACA ARR No. 3K04, 1943.
4. Kotanchik, Joseph N., Woods, Walter, and Weinberger, Robert A.: Investigation of Methods of Supporting Single-Thickness Specimens in a Fixture for Determination of Compressive Stress-Strain Curves. NACA RB No. L5E15, 1945.
5. Heimerl, George J., and Roy, J. Albert: Determination of Desirable Lengths of Z- and Channel-Section Columns for Local-Instability Tests. NACA RB No. L4H10, 1944.

TABLE 1.- COMPRESSIVE PROPERTIES OF 24S-T ALUMINUM-ALLOY SHEET

$$[E_c = 10,700 \text{ ksi}]$$

Columns to which stress-strain curves apply			Stress-strain curve (fig. 9)	Compressive yield stress, σ_{cy}	
Type	Direction of loading	Designation (See tables 2 and 3)		With grain (ksi)	Cross grain (ksi)
Thin strip	With grain and cross grain	All	A	42.9	47.9
Z	With grain	1a to 6a, 6c, 7a, 10a, 10b, 11a to 19a, 26b, 27a, 27c, 28a, 29a, 31b to 32c	B	44.0	46.8
Z	With grain	6b, 7b to 9, 10c, 19b to 26a, 26c, 27b, 28b, 28c, 29b to 31a	C	46.3	51.3
Z	Cross grain	1a to 4c	D	43.4	48.5
Channel	With grain	1 to 6a, 7a, 8a, 9a, 10a, 11a, 12a, 13a, 14a, 15a, 16a, 17a, 18a, 19a, 20a, 21a, 21b, 22a, 23a, 24a, 25a, 27a to 28a, 29a, 30a to 31a, 32a, 33a, 34a, 35a, 36a	E	43.4	48.9
Channel	With grain	6b, 6c, 7b, 7c, 8b, 8c, 9b, 9c, 10b, 10c, 11b, 11c, 12b, 12c, 13b, 13c, 14b, 14c, 15b, 15c, 16b, 16c, 17b, 17c, 18b, 18c, 19b, 19c, 20b, 22b, 23b, 23c, 24b, 24c, 25b, 25c, 26a, 26b, 28b, 29b, 29c, 31b, 32b	F	44.3	49.7
Channel	With grain	31c, 32c, 33b, 33c, 34b, 35b, 36b, 36c	G	43.9	47.9
Channel	Cross grain	1a to 4c	D	43.4	48.5

TABLE 2.- DIMENSIONS AND TEST RESULTS FOR FORMED Z-SECTION
COLUMNS THAT DEVELOP LOCAL INSTABILITY

Column	t (in.)	b _w (in.)	b _F (in.)	L (in.)	L/b _w	b _w /t	b _F /b _w	k _w (a)	$\frac{b_w}{t} \sqrt{\frac{12(1-\mu)^2}{k_w}}$	$\frac{\sigma_{cr}}{\eta}$ (ksi) (b)	σ_{cr} (ksi)	$\bar{\sigma}_{max}$ (ksi)	$\frac{\sigma_{cr}}{\bar{\sigma}_{max}}$
With grain													
1a	0.126	1.92	1.11	9.75	5.1	15.23	0.578	2.33	33.0	97.1	52.4	54.3	0.965
1b	.123	1.88	1.11	7.97	4.3	15.26	.592	2.24	33.7	93.1	53.7	56.5	.951
2a	.126	1.87	1.32	9.75	5.2	14.87	.703	1.68	37.9	73.5	50.5	52.4	.964
2b	.126	1.87	1.32	9.74	5.2	14.85	.703	1.68	37.9	73.7	49.9	51.8	.963
2c	.126	1.87	1.30	9.72	5.2	14.90	.696	1.71	37.7	74.5	49.5	52.4	.945
3a	.122	1.87	1.49	9.60	5.1	15.29	.800	1.35	43.5	55.8	43.1	46.4	.929
3b	.124	1.88	1.49	9.70	5.2	15.14	.793	1.38	42.6	58.2	42.5	45.7	.930
4a	.125	1.88	1.69	9.65	5.2	15.01	.900	1.09	47.5	46.7	40.8	41.8	.976
4b	.126	1.87	1.69	9.71	5.2	14.87	.904	1.09	47.1	47.6	38.8	41.9	.926
4c	.126	1.87	1.70	9.73	5.2	14.87	.909	1.08	47.3	47.2	41.0	43.1	.951
5a	.126	1.86	1.89	9.71	5.2	14.77	1.015	.87	52.4	38.6	34.9	39.5	.883
5b	.126	1.87	1.91	9.60	5.1	14.87	1.017	.86	53.0	37.7	36.2	40.1	.903
5c	.126	1.87	1.90	9.80	5.2	14.87	1.013	.87	52.7	38.1	35.3	39.4	.896
6a	.124	2.41	1.41	10.03	4.2	19.37	.587	2.28	42.4	58.7	44.6	46.9	.951
6b	.123	2.39	1.41	10.04	4.2	19.43	.596	2.21	43.2	56.6	45.7	47.3	.966
6c	.126	2.36	1.45	10.02	4.3	18.71	.613	2.12	42.5	58.5	44.6	47.4	.941
7a	.126	2.37	1.91	12.13	5.1	18.84	.805	1.34	53.8	36.5	32.2	37.9	.850
7b	.126	2.38	1.91	12.22	5.1	18.92	.799	1.35	53.9	36.4	33.7	38.7	.871
7c	.125	2.38	1.90	12.20	5.1	19.01	.799	1.35	54.1	36.1	32.9	38.4	.857
8a	.127	2.36	2.14	12.25	5.2	18.57	.906	1.08	59.1	30.3	30.3	37.0	.819
8b	.127	2.37	2.14	12.16	5.1	18.62	.902	1.09	59.0	30.4	29.1	36.8	.791
8c	.125	2.38	2.15	11.79	5.0	19.05	.904	1.08	60.6	28.8	28.3	36.1	.784
9	.126	2.37	2.39	12.21	5.1	18.84	1.005	.88	66.3	24.0	25.5	35.0	.729

^aFor values of k_w , see figure 2.

$$\frac{b_{\sigma_{cr}}}{\eta} = \frac{k_w \pi^2 E_c t^2}{12(1-\mu^2)b_w^2}, \text{ where } E_c = 10,700 \text{ ksi and } \mu = 0.3.$$

NATIONAL ADVISORY
COMMITTEE FOR AERONAUTICS

TABLE 2.- DIMENSIONS AND TEST RESULTS FOR FORMED Z-SECTION
COLUMNS THAT DEVELOP LOCAL INSTABILITY - Continued

Column	t (in.)	b _w (in.)	b _F (in.)	L (in.)	L/b _w	b _w /t	b _F /b _w	k _w (a)	$\frac{b_w}{t} \sqrt{\frac{12(1-\mu)^2}{k_w}}$	$\frac{\sigma_{cr}}{\eta}$ (ksi) (b)	σ_{cr} (ksi)	$\bar{\sigma}_{max}$ (ksi)	$\frac{\sigma_{cr}}{\bar{\sigma}_{max}}$
With grain													
10a	0.123	2.88	1.75	14.70	5.1	23.43	0.606	2.15	52.8	37.9	34.3	37.0	0.927
10b	.123	2.87	1.74	14.46	5.0	23.35	.606	2.16	52.5	38.3	34.5	36.8	.938
10c	.123	2.88	1.75	14.64	5.1	23.43	.606	2.15	52.8	37.9	34.4	37.7	.912
11a	.125	2.86	2.29	14.56	5.1	22.88	.801	1.35	65.1	24.9	25.0	33.2	.753
11b	.126	2.87	2.30	14.68	5.1	22.81	.801	1.35	64.9	25.1	26.3	33.1	.795
11c	.123	2.88	2.31	14.40	5.0	23.39	.802	1.35	66.5	23.8	25.9	32.5	.797
12a	.126	2.87	2.58	14.70	5.1	22.90	.896	1.10	72.2	20.3	19.7	31.7	.621
12b	.126	2.87	2.56	14.73	5.1	22.85	.890	1.11	71.7	20.6	21.1	31.8	.664
12c	.126	2.88	2.57	14.70	5.1	22.79	.892	1.12	71.2	20.9	22.3	32.0	.697
13a	.123	2.88	2.89	14.72	5.1	23.37	1.003	.88	82.4	15.5	14.7	29.3	.502
13b	.127	2.87	2.88	14.65	5.1	22.71	1.003	.88	80.0	16.5	15.3	30.3	.505
14a	.125	3.38	1.70	17.19	5.1	26.94	.503	2.88	52.5	38.4	32.3	34.1	.946
14b	.127	3.39	1.69	17.15	5.1	26.72	.498	2.90	51.9	39.3	33.6	36.4	.923
14c	.124	3.36	1.69	17.13	5.1	27.10	.504	2.87	52.9	37.3	35.8	37.6	.952
15a	.126	3.38	2.39	17.18	5.1	26.84	.705	1.68	68.4	22.5	21.7	30.8	.705
15b	.126	3.37	2.36	17.14	5.1	26.74	.699	1.70	67.8	23.0	23.7	31.8	.745
15c	.127	3.35	2.36	16.87	5.0	26.46	.704	1.68	67.5	23.2	23.4	30.9	.757
16a	.125	3.37	2.69	17.15	5.1	26.92	.798	1.35	76.6	18.0	17.6	29.2	.603
16b	.127	3.38	2.70	17.20	5.1	26.72	.799	1.35	76.0	18.3	18.0	30.1	.598
17a	.126	3.37	3.03	17.20	5.1	26.64	.899	1.10	84.0	14.9	15.2	27.9	.545
17b	.127	3.37	3.03	17.09	5.1	26.47	.899	1.10	83.4	15.1	16.2	28.6	.566
17c	.128	3.40	3.04	17.23	5.1	26.64	.893	1.12	83.2	15.2	15.4	28.5	.540

^aFor values of k_w, see figure 2.

$$\frac{b\sigma_{cr}}{\eta} = \frac{k_w \pi^2 E_c t^2}{12(1-\mu^2)b_w}, \text{ where } E_c = 10,700 \text{ ksi and } \mu = 0.3.$$

NATIONAL ADVISORY
COMMITTEE FOR AERONAUTICS

TABLE 2.- DIMENSIONS AND TEST RESULTS FOR FORMED Z-SECTION
COLUMNS THAT DEVELOP LOCAL INSTABILITY - Continued

Column	t (in.)	b _W (in.)	b _F (in.)	L (in.)	L/b _W	b _W /t	b _F /b _W	k _W (a)	$\frac{b_W}{t} \sqrt{\frac{12(1-\mu)^2}{k_W}}$	$\frac{\sigma_{cr}}{\eta}$ (ksi) (b)	σ_{cr} (ksi)	$\bar{\sigma}_{max}$ (ksi)	$\frac{\sigma_{cr}}{\bar{\sigma}_{max}}$
With grain													
18a	0.127	3.42	3.39	17.11	5.0	26.97	0.991	0.91	93.4	12.1	10.8	26.9	0.401
18b	.126	3.37	3.37	17.09	5.1	26.88	.999	.90	93.6	12.0	13.6	27.6	.493
18c	.125	3.38	3.38	17.10	5.1	26.91	1.001	.89	94.3	11.9	12.8	26.9	.476
19a	.125	4.04	1.58	20.22	5.0	32.18	.391	3.81	54.5	35.5	32.1	33.5	.958
19b	.125	4.08	1.62	15.80	4.1	32.54	.396	3.78	55.3	34.5	34.0	35.0	.971
19c	.125	4.05	1.59	20.20	5.0	32.45	.392	3.80	55.0	34.9	32.0	34.5	.928
20a	.126	4.02	1.99	19.98	5.0	31.84	.494	2.95	61.3	28.2	27.8	31.0	.897
20b	.122	4.03	2.00	19.88	4.9	32.91	.497	2.93	63.6	26.1	26.1	30.8	.847
21a	.124	4.03	2.39	20.08	5.0	32.44	.594	2.25	71.5	20.7	20.6	29.8	.691
21b	.129	4.01	2.41	19.98	5.0	31.14	.601	2.18	69.7	21.7	20.2	30.0	.673
21c	.127	4.02	2.42	19.93	5.0	31.73	.601	2.18	71.0	20.9	21.7	29.7	.731
22a	.126	4.13	2.79	19.94	4.8	32.85	.676	1.80	80.9	16.2	17.1	27.8	.615
22b	.128	4.04	2.79	20.07	4.3	31.54	.690	1.75	78.8	17.1	18.0	28.1	.641
22c	.124	4.05	2.80	19.99	4.9	32.76	.691	1.73	82.3	15.5	15.9	27.5	.578
23a	.125	4.02	3.18	19.62	4.9	32.18	.793	1.38	90.5	12.9	12.9	26.3	.490
23b	.129	4.04	3.20	19.98	4.9	31.33	.792	1.38	88.2	13.6	13.0	26.6	.489
23c	.127	4.02	3.20	19.93	5.0	31.58	.794	1.37	89.1	13.3	12.5	26.3	.475
24a	.123	4.05	3.61	20.04	4.9	32.85	.892	1.12	102.6	10.0	9.7	24.8	.393
24b	.129	4.00	3.58	19.95	5.0	30.92	.894	1.12	96.5	11.3	10.5	25.6	.410
25a	.126	4.02	4.01	19.82	4.9	31.34	.997	.90	110.9	8.6	8.8	24.0	.365
25b	.126	4.02	4.00	20.02	5.0	32.06	.994	.90	111.5	8.5	8.9	23.7	.376
25c	.129	4.02	4.00	19.85	4.9	31.19	.995	.90	108.7	9.0	10.0	23.9	.417

^aFor values of k_W, see figure 2.

$$\frac{b_{\sigma_{cr}}}{\eta} = \frac{k_W \pi^2 E_c t^2}{12(1-\mu^2)b_W^2}, \text{ where } E_c = 10,700 \text{ ksi and } \mu = 0.3.$$

NATIONAL ADVISORY
COMMITTEE FOR AERONAUTICS

TABLE 2.- DIMENSIONS AND TEST RESULTS FOR FORMED Z-SECTION
COLUMNS THAT DEVELOP LOCAL INSTABILITY - Continued

Column	t (in.)	b _W (in.)	b _F (in.)	L (in.)	L/b _W	b _W /t	b _F /b _W	k _W (a)	$\frac{b_W}{t} \sqrt{\frac{12(1-\mu)^2}{k_W}}$	$\frac{\sigma_{cr}}{\eta}$ (ksi) (b)	σ_{cr} (ksi)	$\bar{\sigma}_{max}$ (ksi)	$\frac{\sigma_{cr}}{\bar{\sigma}_{max}}$
With grain													
26a	0.124	4.88	1.95	24.60	5.1	39.29	0.400	3.74	67.1	23.4	22.2	28.3	0.784
26b	.128	4.87	1.99	24.62	5.1	38.18	.409	3.67	65.8	24.3	23.9	28.0	.854
26c	.124	4.88	1.92	20.30	4.2	39.47	.393	3.78	67.1	23.5	23.9	28.9	.827
27a	.127	4.87	2.45	24.08	4.9	38.52	.502	2.88	75.1	18.8	18.1	26.5	.683
27b	.126	4.92	2.45	24.50	5.0	39.13	.497	2.92	75.7	18.5	18.1	27.6	.656
27c	.129	4.92	2.44	24.51	5.0	38.26	.497	2.92	74.0	19.3	19.3	26.6	.726
28a	.124	4.91	2.99	24.10	4.9	39.54	.609	2.13	89.5	13.2	12.0	24.9	.483
28b	.127	4.87	2.97	24.62	5.1	38.25	.609	2.14	86.4	14.1	13.8	25.8	.535
28c	.125	4.94	2.93	24.50	5.0	39.49	.595	2.23	87.4	13.8	12.4	25.5	.486
29a	.127	4.91	3.41	24.47	5.0	38.62	.695	1.72	97.4	11.1	10.1	23.5	.430
29b	.126	4.90	3.39	24.40	5.0	38.93	.692	1.73	97.8	11.0	10.5	24.2	.434
30a	.129	4.92	3.90	24.75	5.0	38.14	.794	1.37	107.7	9.1	8.9	22.7	.393
30b	.128	4.88	3.91	24.73	5.1	38.22	.802	1.35	108.8	8.9	8.91	23.0	.387
30c	.125	4.89	3.90	24.78	5.1	39.08	.799	1.36	110.7	8.6	8.01	23.0	.348
31a	.126	4.87	4.41	24.70	5.1	38.62	.904	1.08	122.8	7.0	7.1	21.9	.324
31b	.128	4.87	4.41	24.70	5.1	38.15	.905	1.08	121.3	7.2	8.1	21.2	.333
31c	.131	4.92	4.40	24.63	5.0	37.40	.894	1.12	116.8	7.8	6.7	21.7	.311
32a	.129	4.92	4.88	24.61	5.0	38.06	.991	.91	131.8	6.1	6.4	19.9	.320
32b	.125	4.90	4.89	24.54	5.0	39.10	.998	.89	137.0	5.7	6.0	19.9	.301
32c	.124	4.90	4.90	24.45	5.0	39.44	1.000	.89	138.2	5.6	6.1	20.3	.302

^aFor values of k_W , see figure 2.

$$\frac{b_{\sigma_{cr}}}{\eta} = \frac{k_W \pi^2 E_c t^2}{12(1-\mu^2)b_W^2}, \text{ where } E_c = 10,700 \text{ ksi and } \mu = 0.3.$$

NATIONAL ADVISORY
COMMITTEE FOR AERONAUTICS

TABLE 2.- DIMENSIONS AND TEST RESULTS FOR FORMED Z-SECTION
COLUMNS THAT DEVELOP LOCAL INSTABILITY - Concluded

Column	t (in.)	b _w (in.)	b _F (in.)	L (in.)	L/b _w	b _w /t	b _F /b _w	k _w (a)	$\frac{b_w}{t} \sqrt{\frac{12(1-\mu)^2}{k_w}}$	$\frac{\sigma_{cr}}{\eta}$ (ksi) (b)	σ_{cr} (ksi)	$\bar{\sigma}_{max}$ (ksi)	$\frac{\sigma_{cr}}{\bar{\sigma}_{max}}$
Cross grain													
1a	0.105	3.28	1.99	16.51	5.04	31.16	0.607	2.17	69.9	21.6	21.2	29.2	0.726
1b	.105	3.28	1.98	16.50	5.04	31.22	.605	2.18	69.9	21.6	21.4	30.0	.713
2a	.105	2.46	1.48	12.31	5.00	23.45	.600	2.20	52.3	38.7	36.8	38.6	.953
2b	.105	2.47	1.47	12.31	4.99	23.48	.596	2.23	52.0	39.1	35.8	38.5	.930
2c	.105	2.46	1.47	12.31	5.00	23.48	.597	2.22	52.1	39.0	37.4	38.5	.971
3a	.105	2.04	1.21	10.42	5.11	19.43	.592	2.25	42.8	57.6	45.7	47.6	.960
3b	.105	2.05	1.21	10.42	5.09	19.54	.589	2.27	42.9	57.5	46.7	47.6	.981
3c	.105	2.04	1.21	10.42	5.11	19.47	.591	2.27	42.7	57.9	46.4	47.5	.977
4a	.105	1.77	1.05	8.00	4.53	16.81	.596	2.23	37.2	76.3	53.1	54.2	.980
4b	.105	1.77	1.05	7.96	4.51	16.81	.596	2.23	37.2	76.3	50.8	54.1	.939
4c	.105	1.77	1.05	8.00	4.53	16.78	.596	2.23	37.1	76.6	53.1	54.5	.974

^aFor values of k_w, see figure 2.

$$\frac{b_{\sigma_{cr}}}{\eta} = \frac{k_w \pi^2 E_c t^2}{12(1-\mu^2)b_w^2}, \text{ where } E_c = 10,700 \text{ ksi and } \mu = 0.3.$$

NATIONAL ADVISORY
COMMITTEE FOR AERONAUTICS

TABLE 3.- DIMENSIONS AND TEST RESULTS FOR CHANNEL-SECTION COLUMNS THAT DEVELOP LOCAL INSTABILITY

Column	t (in.)	b _W (in.)	b _F (in.)	L (in.)	L/b _W	b _W /t	b _F /b _W	k _W (a)	$\frac{b_W}{t} \sqrt{\frac{12(1-\mu)^2}{k_W}}$	$\frac{\sigma_{cr}}{\eta}$ (ksi) (b)	σ_{cr} (ksi)	$\bar{\sigma}_{max}$ (ksi)	$\frac{\sigma_{cr}}{\bar{\sigma}_{max}}$
With grain													
1	0.104	1.44	0.86	6.02	4.2	13.83	0.601	2.18	30.9	110.0	51.7	56.5	0.915
2a	.105	1.47	1.00	6.04	4.1	13.91	.684	1.76	34.6	87.7	51.0	55.4	.920
2b	.103	1.45	1.00	6.01	4.2	14.00	.691	1.73	35.2	85.3	52.1	53.9	.967
2c	.103	1.46	.99	6.01	4.1	14.10	.683	1.77	35.0	86.1	52.0	55.1	.943
3a	.104	1.46	1.15	7.55	5.2	13.94	.789	1.38	39.2	68.6	45.7	50.3	.909
3b	.105	1.51	1.11	7.63	5.1	14.30	.740	1.54	38.1	72.9	49.3	52.5	.940
4a	.104	1.46	1.31	7.59	5.2	13.95	.898	1.10	44.0	54.5	43.7	46.6	.939
4b	.104	1.47	1.30	7.63	5.2	14.10	.881	1.13	43.8	55.0	42.4	45.8	.926
4c	.104	1.45	1.30	7.54	5.2	13.91	.895	1.11	43.6	55.3	41.3	43.8	.945
5a	.102	1.46	1.43	7.59	5.2	14.31	.984	.92	49.3	43.3	37.0	40.6	.913
5b	.104	1.48	1.42	7.59	5.1	14.25	.959	.97	47.8	46.2	38.9	41.5	.939
5c	.104	1.46	1.43	7.61	5.2	14.00	.988	.91	48.5	44.3	35.8	39.4	.903
6a	.104	2.58	1.03	13.17	5.1	24.80	.397	3.77	42.2	59.4	44.8	47.1	.953
6b	.105	2.57	1.02	13.20	5.2	24.45	.397	3.76	41.7	60.9	46.5	48.8	.953
6c	.105	2.57	1.02	13.22	5.2	24.40	.398	3.76	41.6	61.1	46.5	48.3	.963
7a	.104	2.59	1.27	13.19	5.1	24.80	.490	2.98	47.5	46.9	37.5	41.3	.909
7b	.105	2.59	1.27	13.15	5.1	24.70	.490	2.98	47.3	47.2	38.1	42.0	.906
7c	.105	2.57	1.27	13.22	5.1	24.41	.493	2.96	46.9	47.3	38.3	41.7	.918
8a	.104	2.59	1.53	13.17	5.1	24.80	.589	2.26	54.5	35.4	31.4	35.2	.893
8b	.105	2.55	1.53	13.12	5.2	24.20	.598	2.20	53.9	36.2	31.0	36.0	.861
8c	.106	2.55	1.53	13.14	5.2	24.15	.598	2.20	53.8	36.5	31.3	36.2	.864
9a	.104	2.59	1.78	13.09	5.1	24.80	.688	1.74	62.2	27.4	26.7	33.3	.803
9b	.106	2.58	1.75	13.14	5.1	24.40	.678	1.79	60.3	28.2	26.4	34.1	.774
9c	.105	2.58	1.76	13.12	5.1	24.50	.681	1.76	61.0	28.7	26.4	33.8	.781

^aFor values of k_W, see figure 2.

$$\frac{\sigma_{cr}}{\eta} = \frac{k_W \pi^2 E_c t^2}{12(1-\mu^2)b_W^2}, \text{ where } E_c = 10,700 \text{ ksi and } \mu = 0.3.$$

NATIONAL ADVISORY
COMMITTEE FOR AERONAUTICS

TABLE 3.- DIMENSIONS AND TEST RESULTS FOR CHANNEL-SECTION
COLUMNS THAT DEVELOP LOCAL INSTABILITY - Continued

Column	t (in.)	b _w (in.)	b _F (in.)	L (in.)	L/b _w	b _w /t	b _F /b _w	k _w (a)	$\frac{b_w}{t} \sqrt{\frac{12(1-\mu)^2}{k_w}}$	$\frac{\sigma_{cr}}{\eta}$ (ksi) (b)	σ_{cr} (ksi)	$\bar{\sigma}_{max}$ (ksi)	$\frac{\sigma_{cr}}{\bar{\sigma}_{max}}$
With grain													
10a	0.104	2.59	2.01	13.12	5.1	24.84	0.777	1.41	69.2	22.1	22.6	31.4	0.720
10b	.104	2.57	2.01	13.14	5.1	24.60	.781	1.41	68.5	22.5	22.7	31.9	.711
10c	.105	2.57	2.02	13.19	5.1	24.48	.785	1.40	68.4	22.6	21.2	32.3	.657
11a	.104	2.01	2.28	13.14	5.0	25.03	.875	1.15	77.2	17.8	15.8	30.4	.520
11b	.105	2.58	2.28	13.18	5.1	24.43	.885	1.13	76.0	18.3	18.7	30.6	.611
11c	.105	2.56	2.30	13.14	5.1	24.33	.901	1.09	77.0	17.8	16.6	30.2	.548
12a	.104	2.61	2.56	13.13	5.0	25.11	.980	.93	86.1	14.2	15.2	28.8	.530
12b	.105	2.58	2.55	13.19	5.1	24.62	.938	.915	85.0	14.6	14.2	29.1	.487
12c	.105	2.56	2.56	13.20	5.2	24.29	1.001	.90	84.6	14.7	13.0	29.2	.445
13a	.103	3.03	.93	15.61	5.2	29.32	.308	4.36	46.4	49.1	38.3	41.1	.933
13b	.104	3.07	.92	15.66	5.1	29.53	.298	4.41	46.5	48.9	38.7	42.2	.917
13c	.105	3.07	.93	15.67	5.1	29.18	.303	4.38	46.1	49.8	41.2	43.2	.954
14a	.104	3.07	1.23	15.66	5.1	29.48	.400	3.74	50.4	41.6	36.7	38.5	.952
14b	.105	3.08	1.22	15.66	5.1	29.29	.398	3.75	50.0	42.3	37.5	39.1	.958
14c	.104	3.09	1.22	15.64	5.1	29.64	.394	3.79	50.3	41.7	36.1	38.5	.937
15a	.104	3.06	1.54	15.69	5.1	29.46	.502	2.88	57.4	32.1	31.1	32.6	.955
15b	.105	3.09	1.54	15.63	5.1	29.38	.499	2.91	56.9	32.6	29.4	33.1	.886
15c	.106	3.06	1.53	15.67	5.1	29.04	.500	2.90	56.4	33.2	29.1	33.9	.856
16a	.104	3.07	1.85	15.66	5.1	29.45	.604	2.17	66.1	24.2	23.1	30.3	.762
16b	.106	3.11	1.83	15.65	5.0	29.38	.583	2.27	64.4	25.4	23.7	31.8	.745
16c	.105	3.10	1.86	15.66	5.1	29.48	.600	2.20	65.6	24.5	23.7	31.7	.749
17a	.105	3.08	2.15	15.67	5.1	29.48	.698	1.71	74.5	19.0	19.0	29.3	.648
17b	.105	3.11	2.12	15.64	5.0	29.46	.684	1.77	73.2	19.7	18.3	29.8	.613
17c	.106	3.09	2.14	15.66	5.1	29.33	.692	1.73	73.7	19.5	17.5	30.8	.570

^aFor values of k_w, see figure 2.

$$\frac{\sigma_{cr}}{\eta} = \frac{k_w \pi^2 E_c t^2}{12(1-\mu^2)b_w^2}, \text{ where } E_c = 10,700 \text{ ksi and } \mu = 0.3.$$

NATIONAL ADVISORY
COMMITTEE FOR AERONAUTICS

TABLE 3.- DIMENSIONS AND TEST RESULTS FOR CHANNEL-SECTION
COLUMNS THAT DEVELOP LOCAL INSTABILITY - Continued

Column	t (in.)	b _w (in.)	b _F (in.)	L (in.)	L/b _w	b _w /t	b _F /b _w	k _w (a)	$\frac{b_w}{t} \sqrt{\frac{12(1-\mu)^2}{k_w}}$	$\frac{\sigma_{cr}}{\eta}$ (ksi) (b)	σ_{cr} (ksi)	$\bar{\sigma}_{max}$ (ksi)	$\frac{\sigma_{cr}}{\bar{\sigma}_{max}}$
With grain													
18a	0.104	3.07	2.44	15.67	5.1	29.64	0.796	1.37	83.7	15.0	13.8	27.8	0.496
18b	.105	3.11	2.45	15.66	5.0	29.62	.787	1.39	83.0	15.3	14.8	28.8	.513
18c	.104	3.10	2.45	15.66	5.1	29.79	.788	1.39	83.4	15.1	13.0	29.0	.448
19a	.105	3.09	2.76	15.67	5.1	29.52	.894	1.11	92.6	12.3	13.7	26.7	.513
19b	.105	3.11	2.75	15.66	5.0	29.54	.885	1.13	91.8	12.5	12.6	26.9	.468
19c	.106	3.12	2.76	15.66	5.0	29.54	.885	1.13	91.8	12.5	12.6	27.1	.465
20a	.104	3.11	3.06	15.65	5.0	29.91	.983	.92	103.1	9.9	9.1	25.4	.358
20b	.104	3.13	3.06	15.71	5.0	30.06	.979	.93	102.9	10.0	10.2	25.0	.408
21a	.103	3.58	1.08	18.19	5.1	34.66	.303	4.39	54.6	35.3	32.6	34.2	.953
21b	.105	3.58	1.08	18.13	5.1	34.10	.302	4.39	53.8	36.5	33.7	35.5	.949
22a	.104	3.59	1.44	18.10	5.0	34.53	.402	3.72	59.2	30.2	28.4	30.1	.943
22b	.105	3.63	1.45	18.10	5.0	34.56	.399	3.74	59.0	30.3	30.5	31.7	.962
23a	.104	3.62	1.79	18.19	5.0	34.65	.493	2.95	66.6	23.7	22.8	28.4	.803
23b	.106	3.59	1.79	18.15	5.0	33.86	.499	2.90	65.7	24.4	23.0	28.6	.804
23c	.106	3.60	1.81	18.15	5.0	34.00	.502	2.88	66.2	24.1	22.3	29.8	.748
24a	.105	3.61	2.15	18.15	5.0	34.40	.596	2.22	76.3	18.2	16.5	27.5	.600
24b	.106	3.62	2.13	18.13	5.0	34.08	.588	2.28	74.8	19.0	16.9	28.3	.597
24c	.105	3.62	2.15	18.15	5.0	34.44	.593	2.25	76.2	18.4	17.5	28.4	.616
25a	.105	3.61	2.51	18.17	5.0	34.33	.697	1.71	86.8	14.0	13.0	26.0	.498
25b	.106	3.60	2.50	18.18	5.0	34.05	.694	1.73	85.8	14.4	14.9	25.9	.575
25c	.104	3.56	2.55	18.17	5.1	34.11	.717	1.63	88.3	13.5	14.4	26.6	.541
26a	.105	3.63	2.87	18.16	5.0	34.52	.792	1.37	97.4	11.1	10.0	25.2	.397
26b	.105	3.60	2.87	18.16	5.1	34.14	.798	1.36	96.8	11.3	10.4	25.3	.411

^aFor values of k_w , see figure 2.

$$\frac{b_{\sigma_{cr}}}{\eta} = \frac{k_w \pi^2 E_c t^2}{12(1-\mu^2)b_w^2}, \text{ where } E_c = 10,700 \text{ ksi and } \mu = 0.3.$$

NATIONAL ADVISORY
COMMITTEE FOR AERONAUTICS

TABLE 3.- DIMENSIONS AND TEST RESULTS FOR CHANNEL-SECTION
COLUMNS THAT DEVELOP LOCAL INSTABILITY - Continued

Column	t (in.)	b _w (in.)	b _F (in.)	L (in.)	L/b _w	b _w /t	b _F /b _w	k _w (a)	$\frac{b_w}{t} \sqrt{\frac{12(1-\mu)^2}{k_w}}$	$\frac{\sigma_{cr}}{\eta}$ (ksi) (b)	σ_{cr} (ksi)	$\bar{\sigma}_{max}$ (ksi)	$\frac{\sigma_{cr}}{\bar{\sigma}_{max}}$
With grain													
27a	0.104	3.60	3.22	18.10	5.0	34.46	0.894	1.11	108.1	9.1	9.6	23.0	0.417
27b	.105	3.55	3.22	18.15	5.1	33.68	.906	1.09	106.6	9.3	8.7	25.0	.349
27c	.105	3.62	3.22	18.13	5.0	34.57	.888	1.13	107.4	9.2	8.9	23.3	.381
28a	.105	3.56	3.58	18.14	5.1	33.86	1.007	.87	119.9	7.4	5.7	21.5	.266
28b	.106	3.63	3.57	18.15	5.0	34.37	.984	.93	117.7	7.6	7.9	22.3	.357
29a	.103	4.50	1.35	22.63	5.0	43.87	.299	4.41	69.0	22.2	21.2	26.0	.815
29b	.106	4.47	1.36	22.63	5.1	42.21	.303	4.38	66.7	23.7	23.7	27.2	.871
29c	.104	4.53	1.38	22.64	5.0	43.48	.306	4.37	68.7	22.3	23.0	27.3	.842
30a	.103	4.52	1.81	22.53	5.0	43.78	.400	3.74	74.8	18.9	17.9	25.2	.710
30b	.105	4.50	1.81	22.65	5.0	42.71	.403	3.71	73.3	19.7	19.2	25.9	.741
30c	.106	4.50	1.81	22.66	5.0	42.51	.401	3.73	72.8	20.0	20.0	27.4	.730
31a	.104	4.51	2.27	22.48	5.0	43.48	.503	2.87	84.8	14.6	13.6	24.4	.557
31b	.105	4.54	2.25	22.65	5.0	43.11	.496	2.93	83.2	15.2	15.1	24.7	.613
31c	.105	4.50	2.27	22.63	5.0	42.95	.505	2.85	84.0	14.9	14.6	25.1	.582
32a	.104	4.52	2.70	22.60	5.0	43.22	.598	2.21	96.1	11.4	10.5	23.0	.457
32b	.105	4.53	2.68	22.72	5.0	43.14	.591	2.25	95.1	11.7	10.0	23.7	.422
32c	.105	4.52	2.70	22.60	5.0	43.21	.598	2.20	96.2	11.4	10.8	23.3	.464
33a	.104	4.55	3.17	22.51	5.0	43.71	.698	1.70	110.8	8.6	7.8	21.0	.373
33b	.105	4.52	3.16	22.73	5.0	43.05	.699	1.70	109.1	8.9	7.2	22.2	.326
33c	.105	4.54	3.16	22.73	5.0	43.20	.696	1.71	109.1	8.9	7.9	22.9	.345
34a	.104	4.55	3.59	22.63	5.0	43.75	.789	1.38	123.1	7.0	7.1	20.0	.355
34b	.104	4.56	3.59	22.63	5.0	43.61	.788	1.38	122.7	7.0	6.9	20.8	.333
35a	.104	4.56	4.03	22.61	5.0	43.72	.884	1.13	135.9	5.8	4.9	19.0	.258
35b	.106	4.54	4.12	22.70	5.0	42.90	.908	1.08	136.4	5.7	5.0	19.6	.255
36a	.104	4.54	4.48	22.65	5.0	43.66	.987	.91	151.3	4.6	4.7	18.0	.263
36b	.105	4.51	4.53	22.64	5.0	43.05	1.006	.88	151.6	4.5	4.2	18.5	.226
36c	.106	4.51	4.52	22.60	5.0	42.62	1.002	.89	149.4	4.7	4.5	19.1	.236

^aFor values of k_w, see figure 2.

$$\frac{b\sigma_{cr}}{\eta} = \frac{k_w \eta^2 E_c t^2}{12(1-\mu^2)b_w^2}, \text{ where } E_c = 10,700 \text{ ksi and } \mu = 0.3.$$

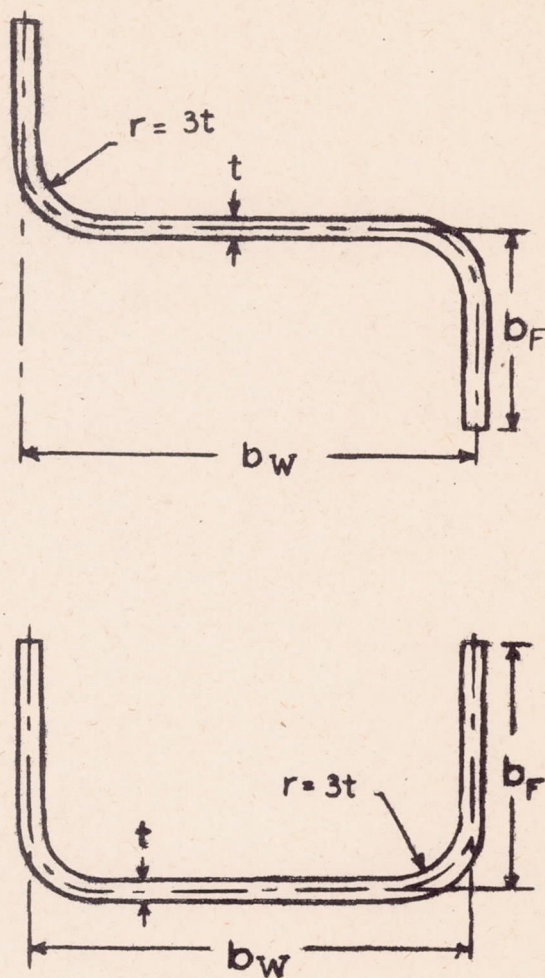
TABLE 3.- DIMENSIONS AND TEST RESULTS FOR CHANNEL-SECTION
COLUMNS THAT DEVELOP LOCAL INSTABILITY - Concluded

Column	t (in.)	b _w (in.)	b _F (in.)	L (in.)	L/b _w	b _w /t	b _F /b _w	k _w (a)	$\frac{b_w}{t} \sqrt{\frac{12(1-\mu)^2}{k_w}}$	$\frac{\sigma_{cr}}{\eta}$ (ksi) (b)	σ_{cr} (ksi)	$\bar{\sigma}_{max}$ (ksi)	$\frac{\sigma_{cr}}{\bar{\sigma}_{max}}$
Cross grain													
1a	0.105	3.30	1.98	16.50	5.0	31.35	0.602	2.19	70.0	21.5	21.8	30.2	0.723
1b	.105	3.31	1.98	16.50	5.0	31.63	.599	2.20	70.5	21.3	21.5	30.0	.716
1c	.106	3.30	1.98	16.48	5.0	31.28	.600	2.20	69.7	21.7	22.3	30.2	.739
2a	.105	2.49	1.47	12.31	4.9	23.76	.590	2.28	52.0	39.1	36.3	38.6	.951
2b	.105	2.48	1.48	12.31	5.0	23.67	.597	2.22	52.5	38.3	36.2	38.5	.941
2c	.105	2.47	1.48	12.32	5.0	23.55	.598	2.22	52.2	38.7	37.4	39.1	.957
3a	.105	2.00	1.21	10.39	5.2	19.04	.605	2.18	42.6	58.2	44.9	47.1	.954
3b	.105	2.00	1.20	10.40	5.2	19.14	.601	2.20	42.7	58.0	44.6	47.4	.941
3c	.104	2.00	1.21	10.41	5.2	19.12	.604	2.18	42.8	57.7	44.6	46.5	.959
4a	.106	1.76	1.05	7.97	4.5	16.71	.592	2.25	36.8	77.9	51.4	53.2	.966
4b	.106	1.76	1.06	8.00	4.5	16.69	.598	2.22	37.0	77.0	51.4	53.0	.970
4c	.106	1.77	1.04	8.00	4.5	16.73	.591	2.27	36.7	78.5	50.7	53.4	.949

^aFor values of k_w , see figure 2.

$$\frac{b\sigma_{cr}}{\eta} = \frac{k_w \pi^2 E_c t^2}{12(1-\mu^2)b_w^2}, \text{ where } E_c = 10,700 \text{ ksi and } \mu = 0.3.$$

NATIONAL ADVISORY
COMMITTEE FOR AERONAUTICS



NATIONAL ADVISORY
COMMITTEE FOR AERONAUTICS

Figure 1. - Cross sections of Z- and channel-section columns.

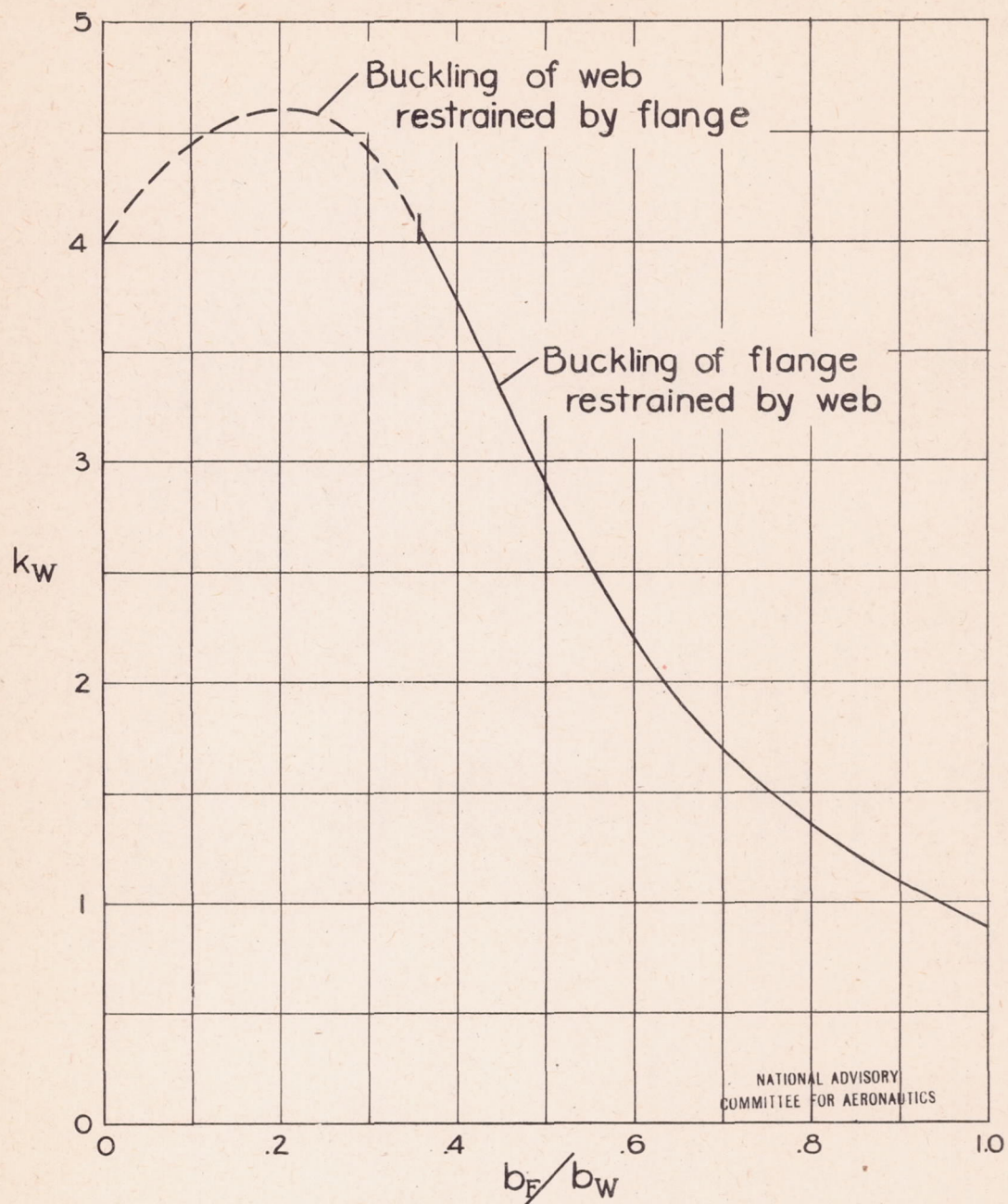
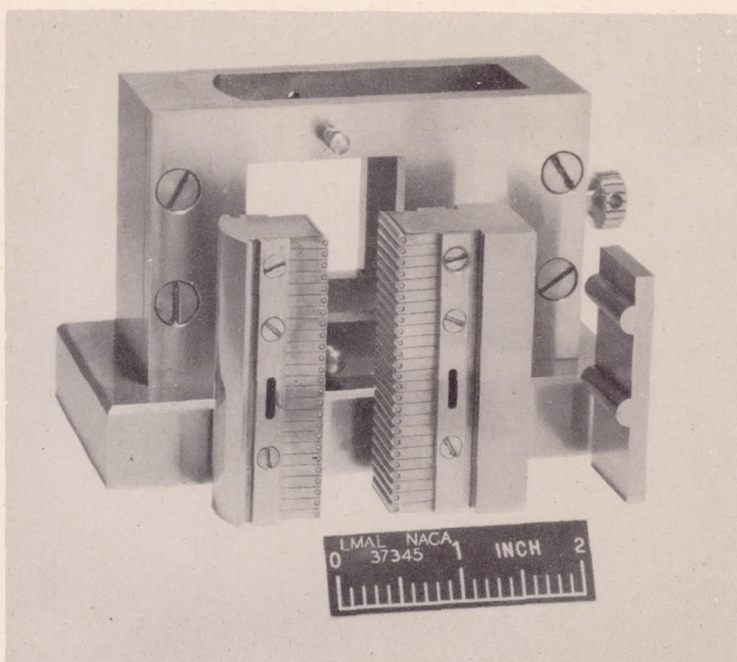
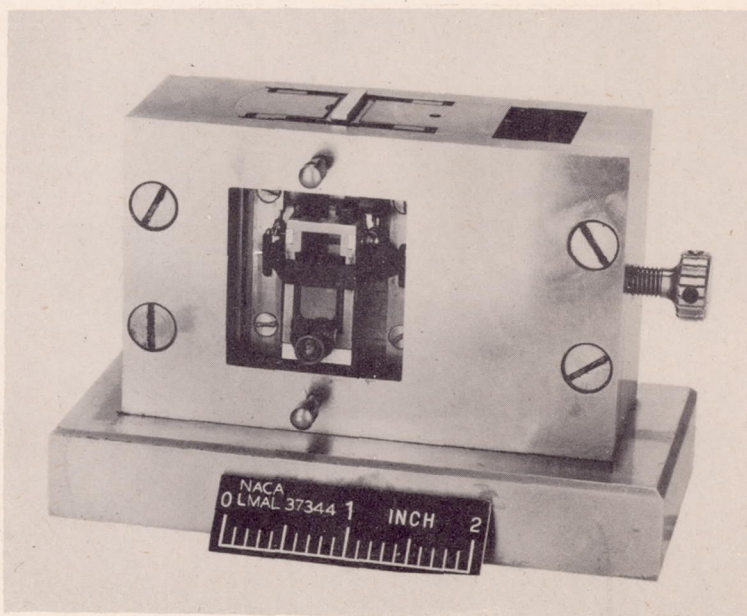


Figure 2.-Values of k_w for Z- and channel-section columns of uniform thickness (from reference 3).

$$\frac{\sigma_{cr}}{\eta} = \frac{k_w \pi^2 E_c t^2}{12(1-\mu^2)b_w^2}$$

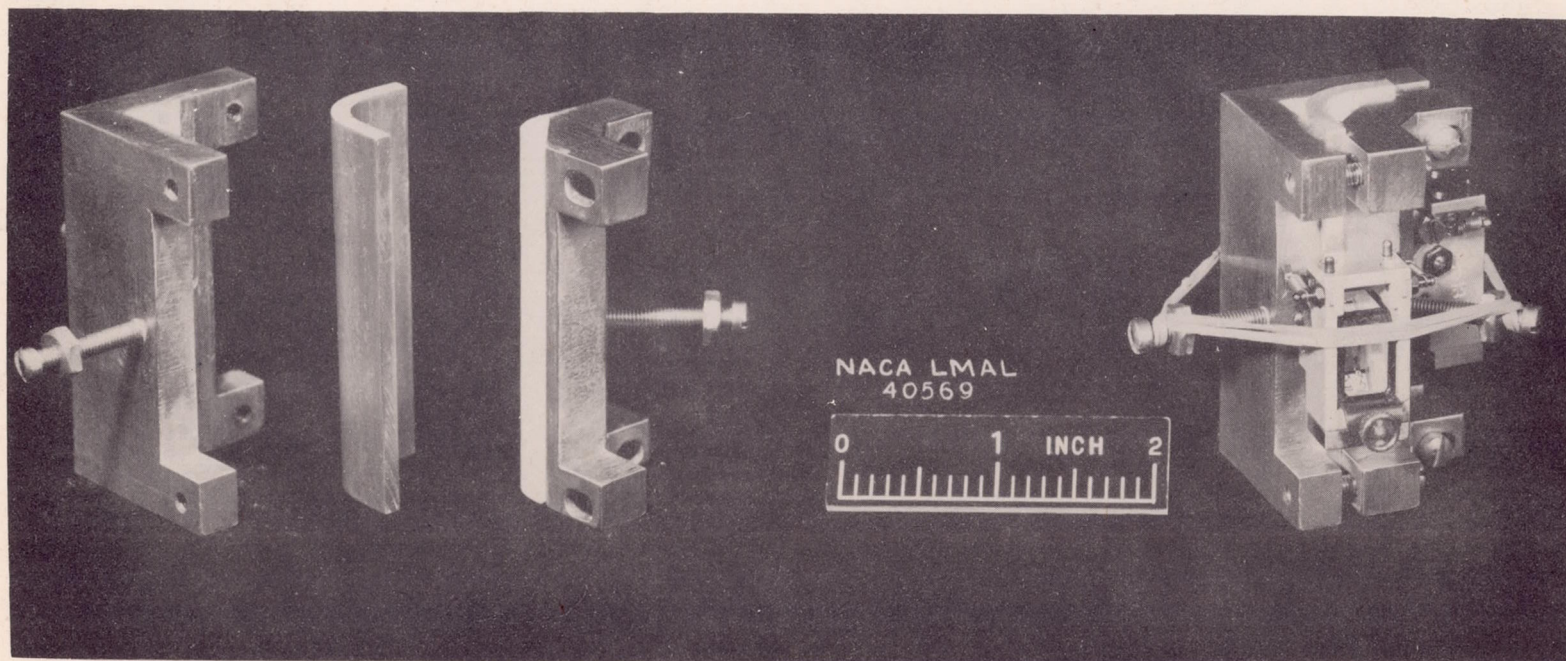


(a) Unassembled.



(b) Assembled with Tuckerman optical strain gage in place on specimen.

Figure 3.- Fixture for obtaining compressive stress-strain curves of flat sheet.



(a) Unassembled.

(b) Assembled with Tuckerman optical strain gage attached.

Figure 4.- Fixture for obtaining compressive stress-strain curve of bent material from corner of Z- or channel-section column.

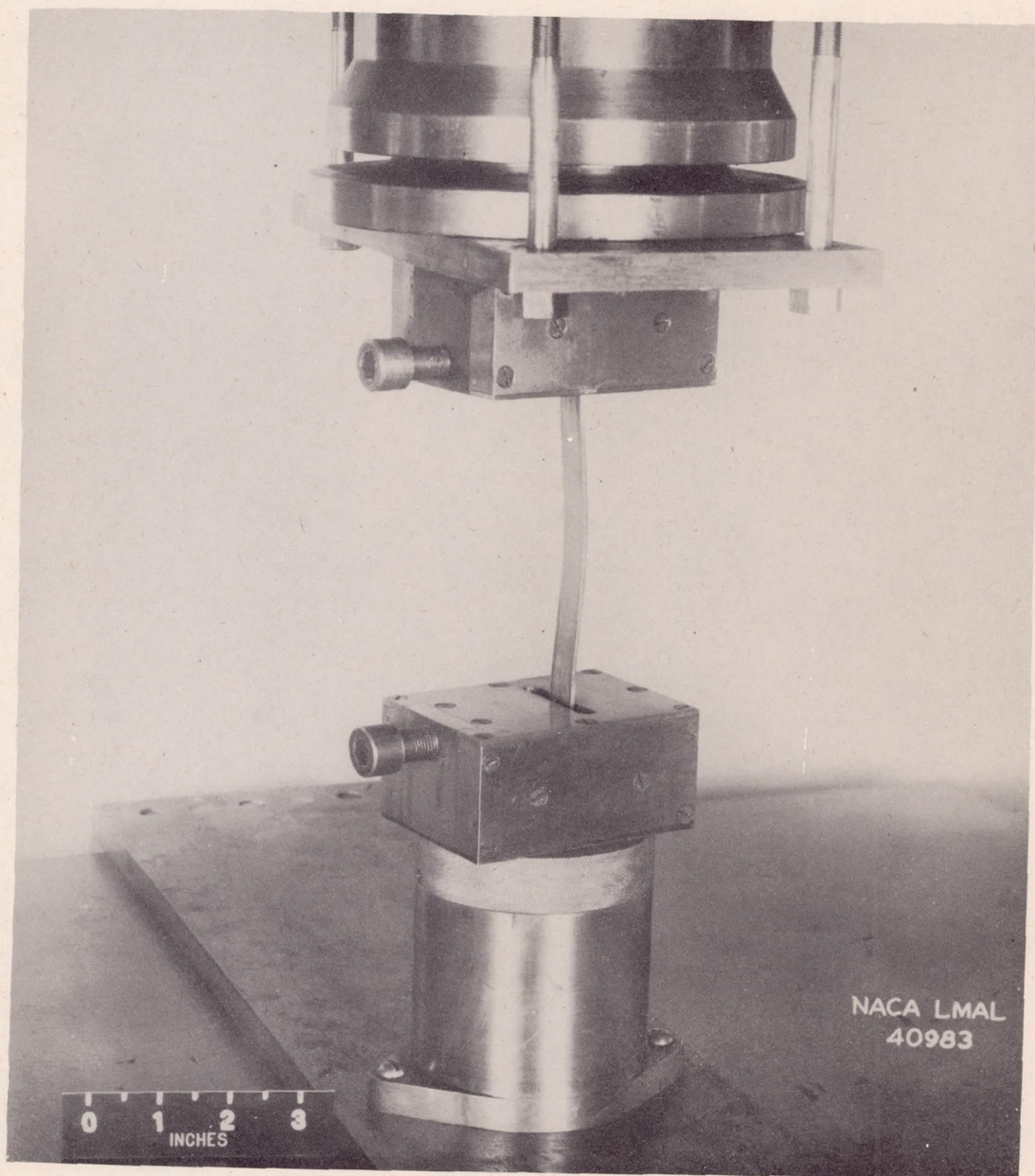
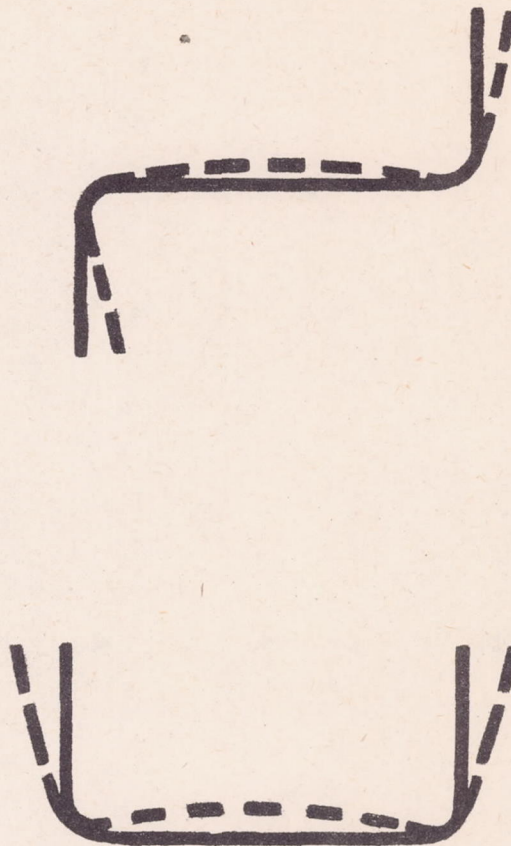


Figure 5.- End fixtures and setup for thin-strip column tests.



NATIONAL ADVISORY
COMMITTEE FOR AERONAUTICS

Figure 6.- Typical cross-sectional distortion
of columns that develop local instability.

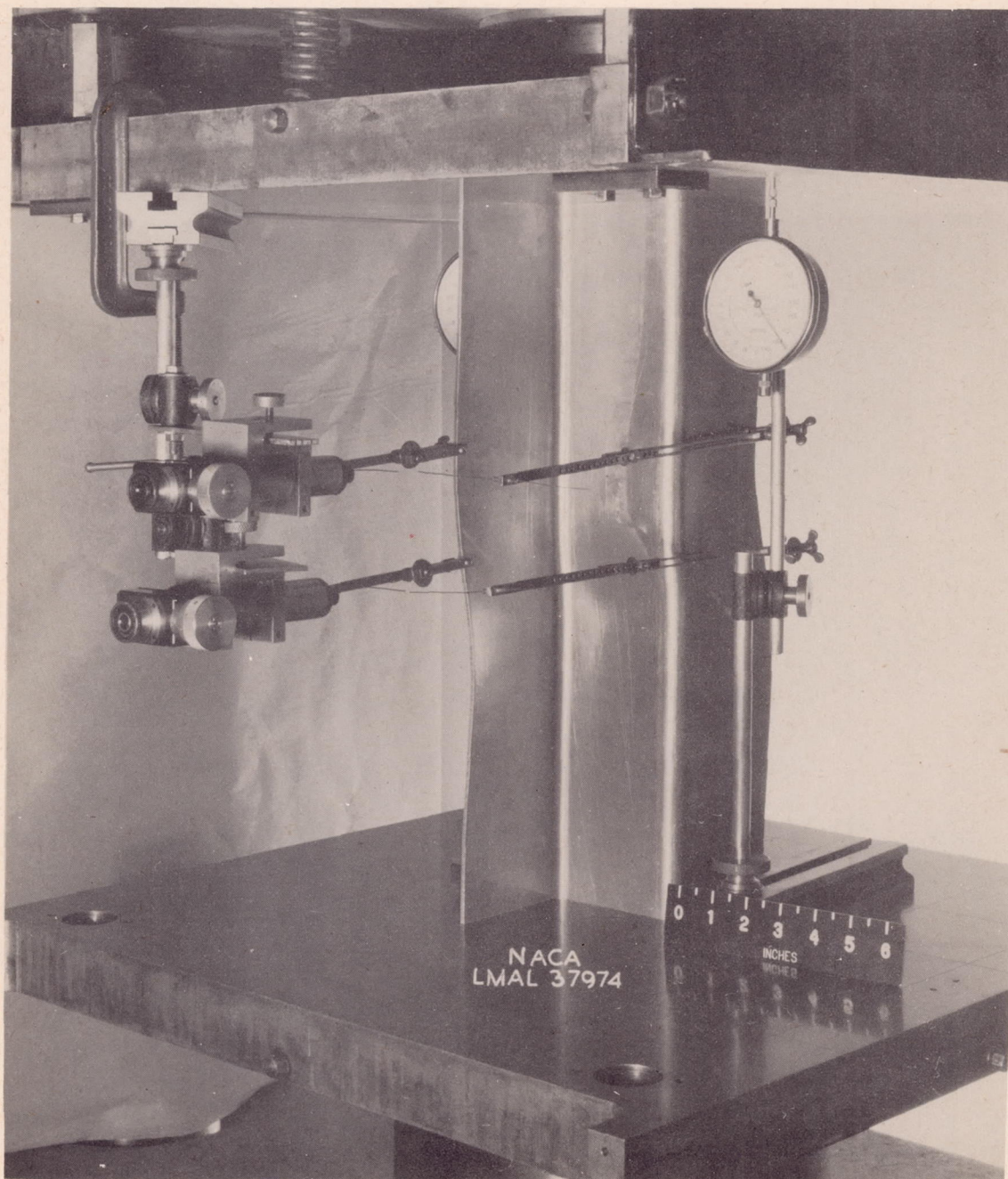


Figure 7.- Z-section column under test for study of instability of plates.

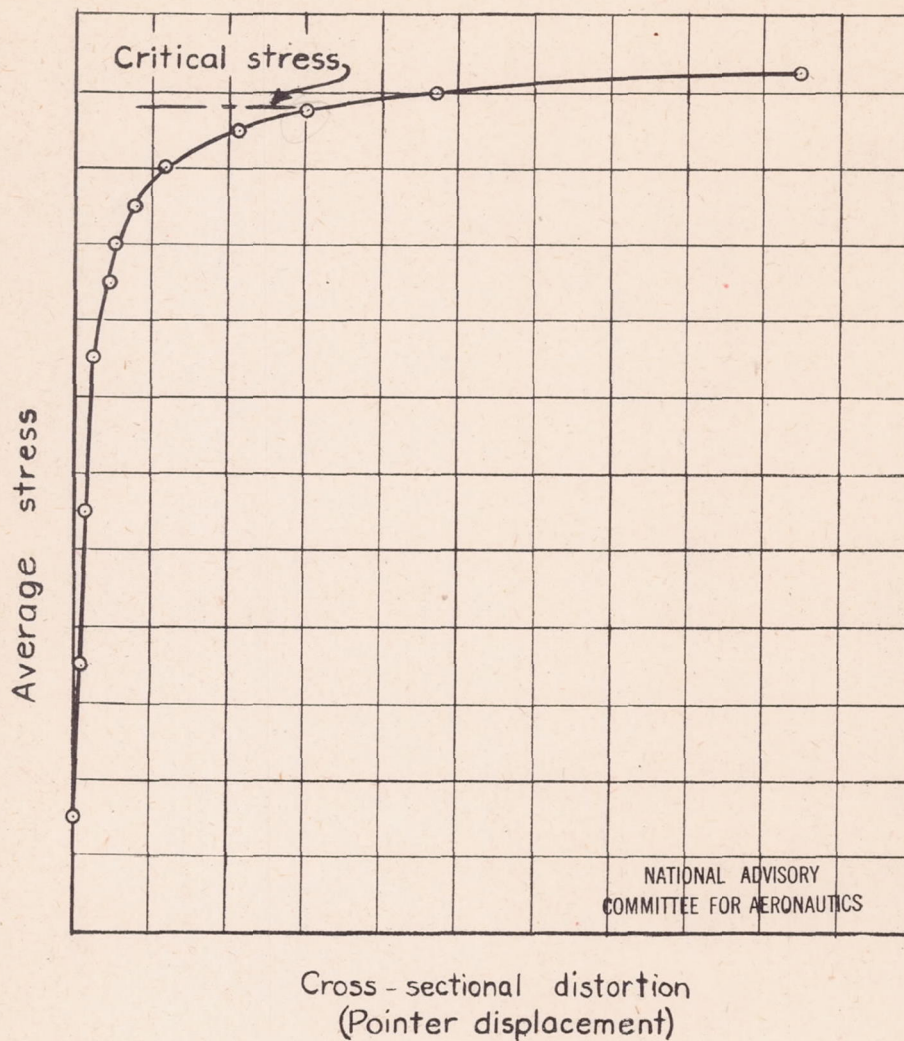


Figure 8.- Illustrative stress-distortion curve for determination of critical stress for Z- or channel-section columns loaded in compression.

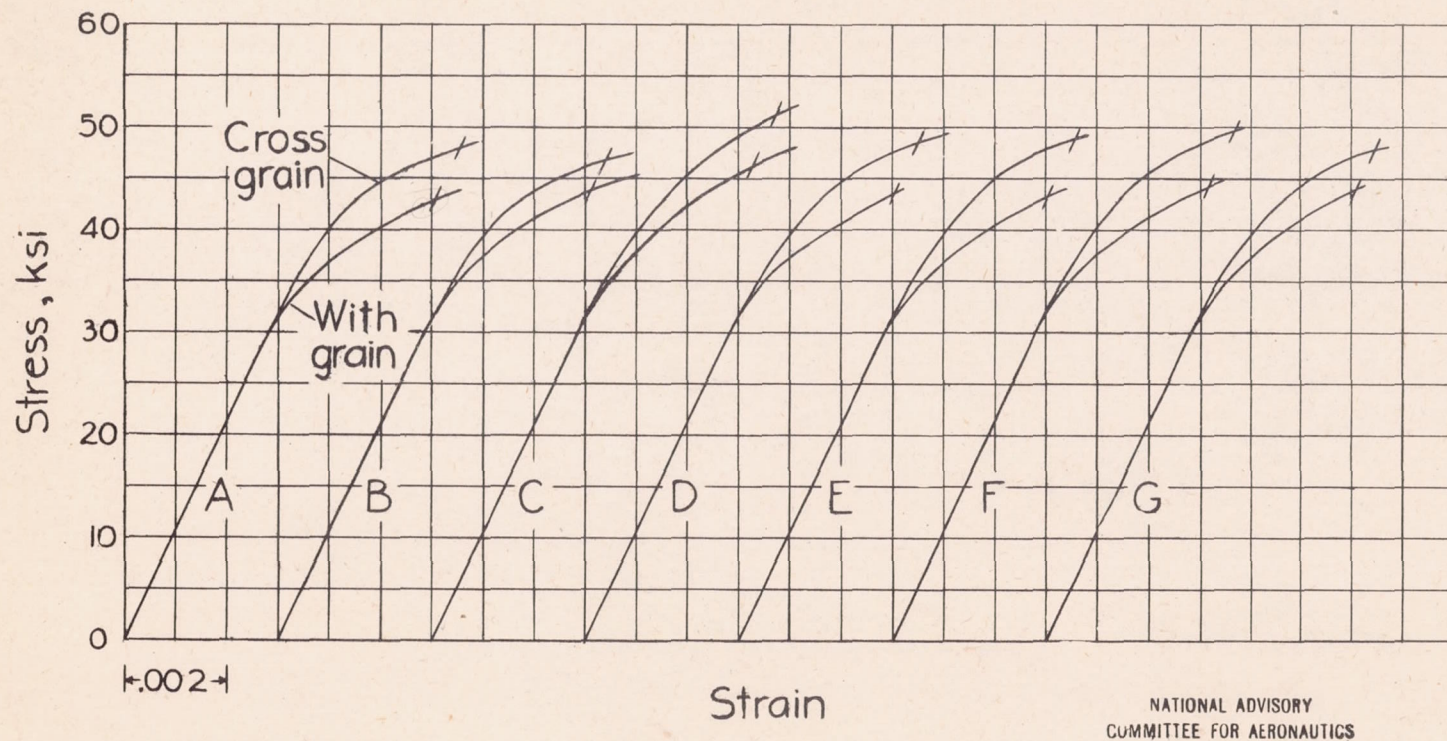


Figure 9. - Compressive stress-strain curves for 24S-T aluminum-alloy flat sheet.
(Curves A, B, C, etc. are identified in table 1.)

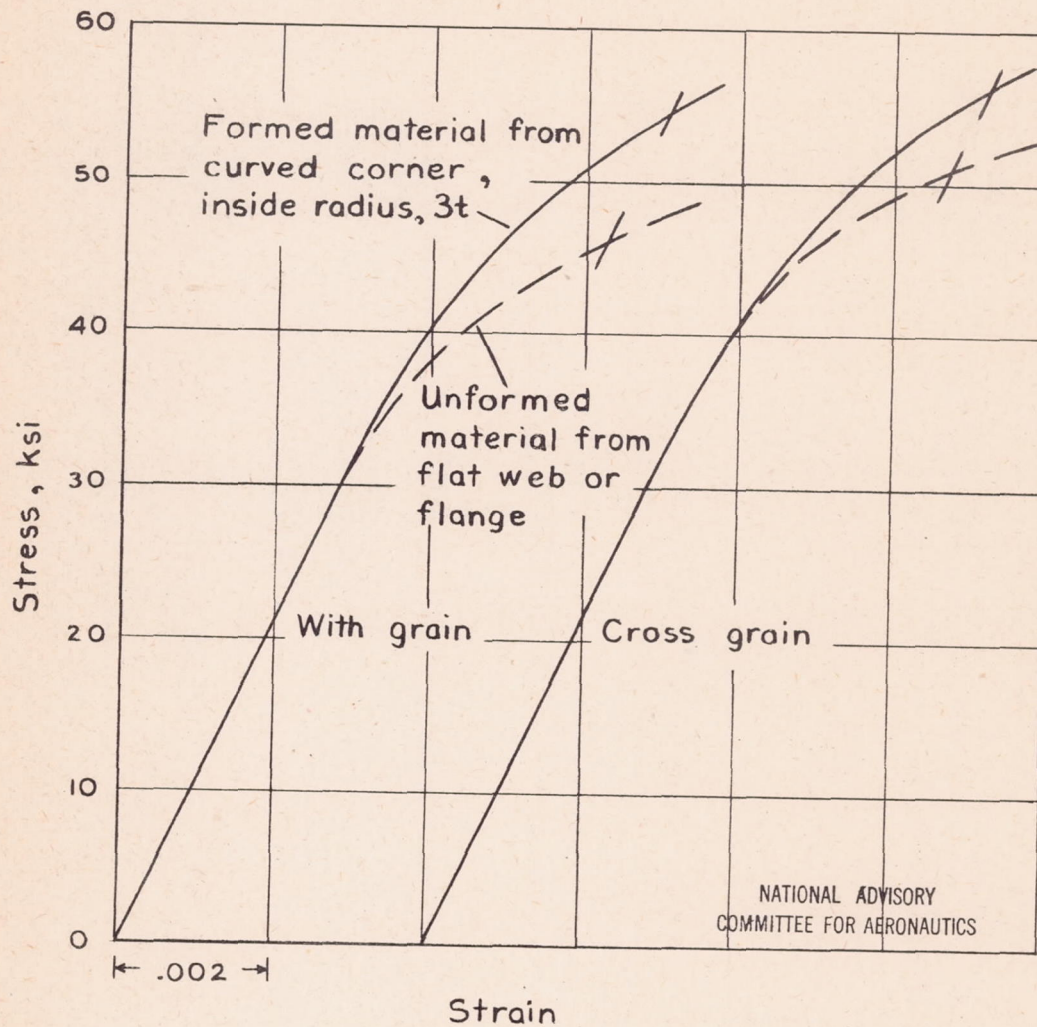


Figure 10.- Effect of forming on compressive stress-strain curves for 24S-T aluminum-alloy Z-section; $t = 0.125$ inches.

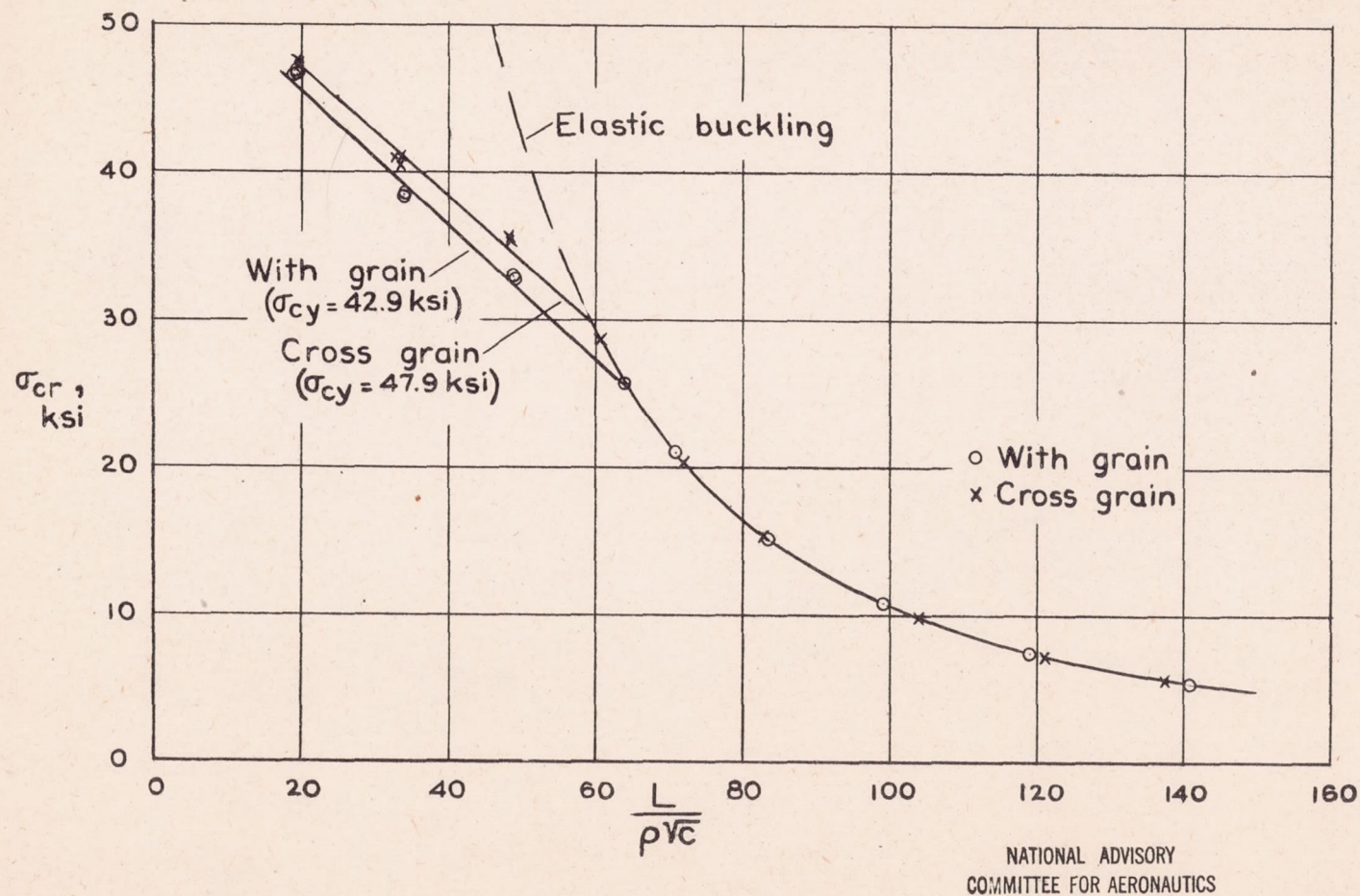


Figure 11. - Column curves for 24S-T aluminum-alloy sheet.

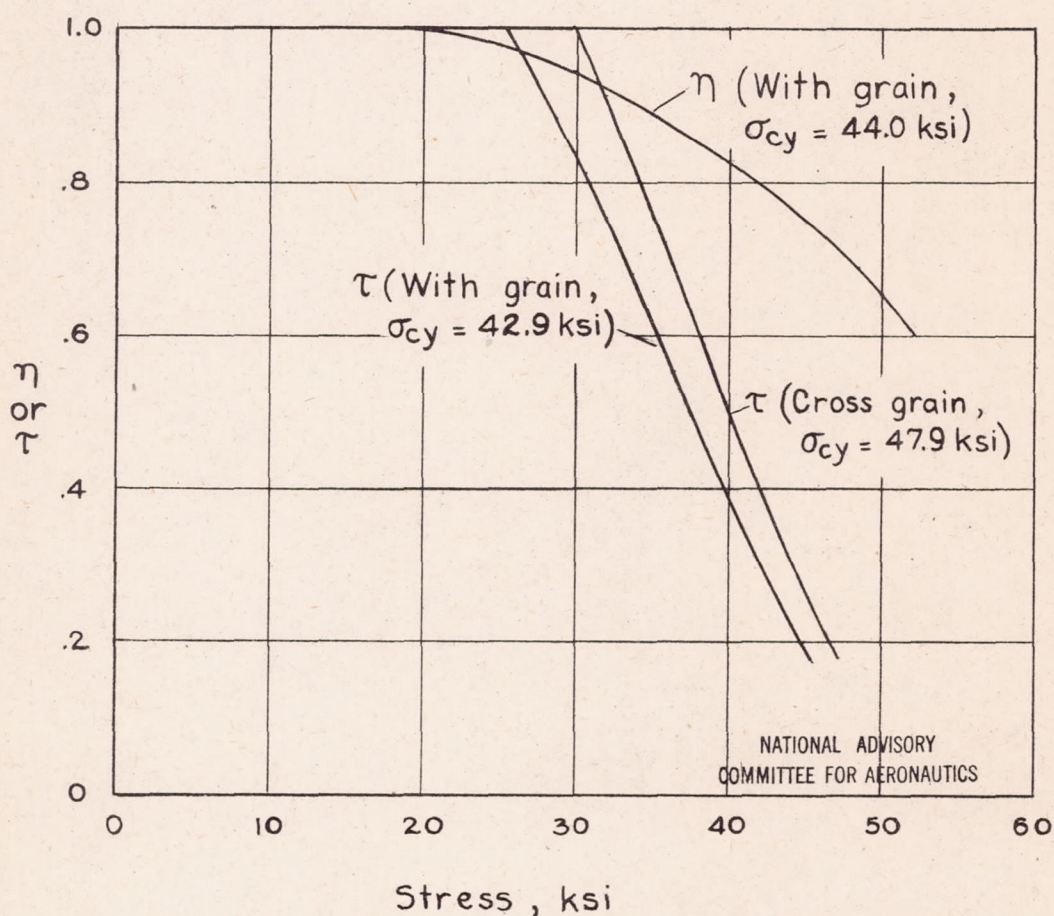


Figure 12.- Variation of τ and η with stress for 24S-T aluminum-alloy sheet. (η obtained from tests of formed columns.)

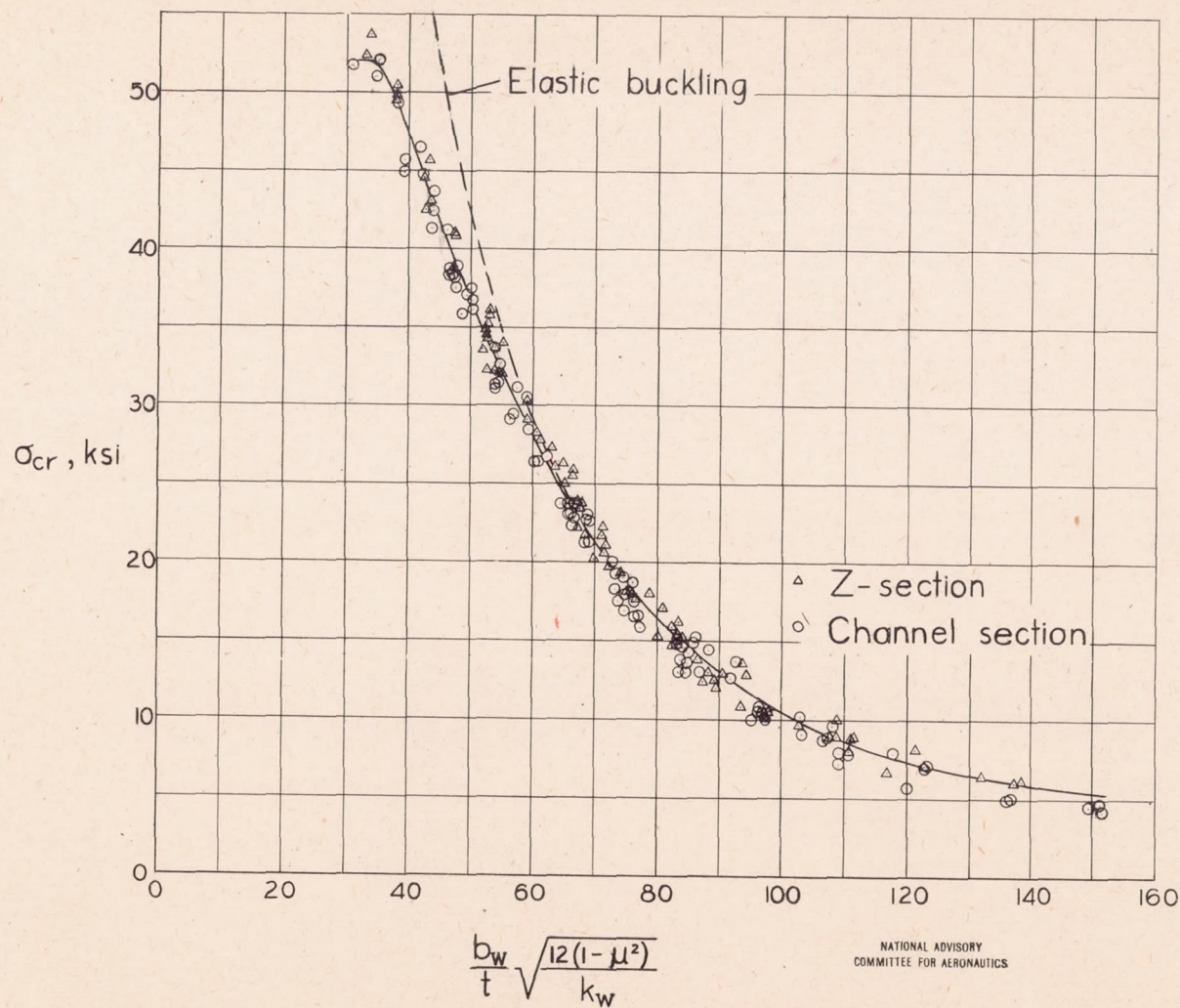


Figure 13.-Plate-buckling curve for 245-T aluminum-alloy sheet loaded in the with-grain direction, obtained from tests of formed columns; $\sigma_{cy}=44\text{ksi}$.

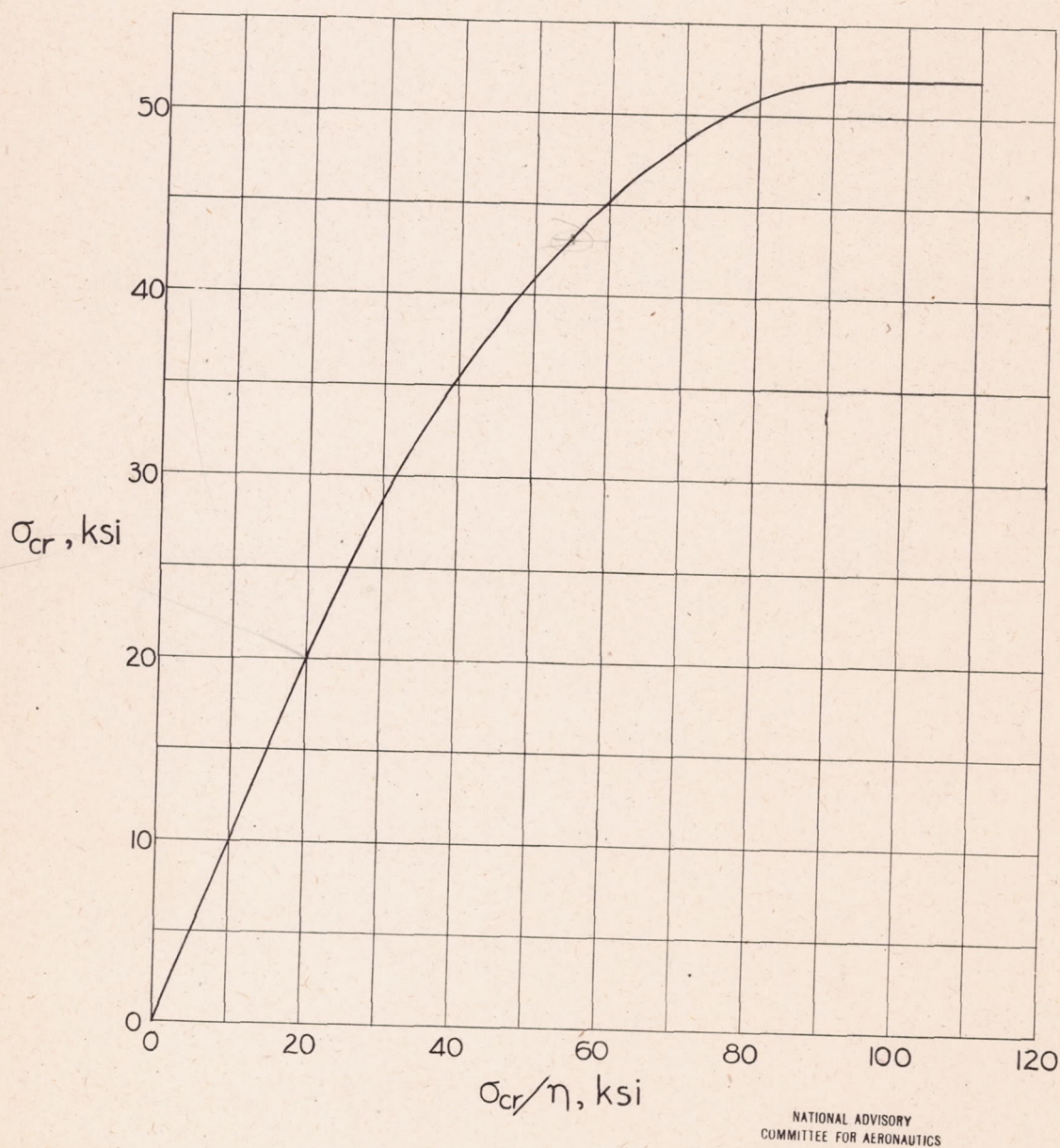
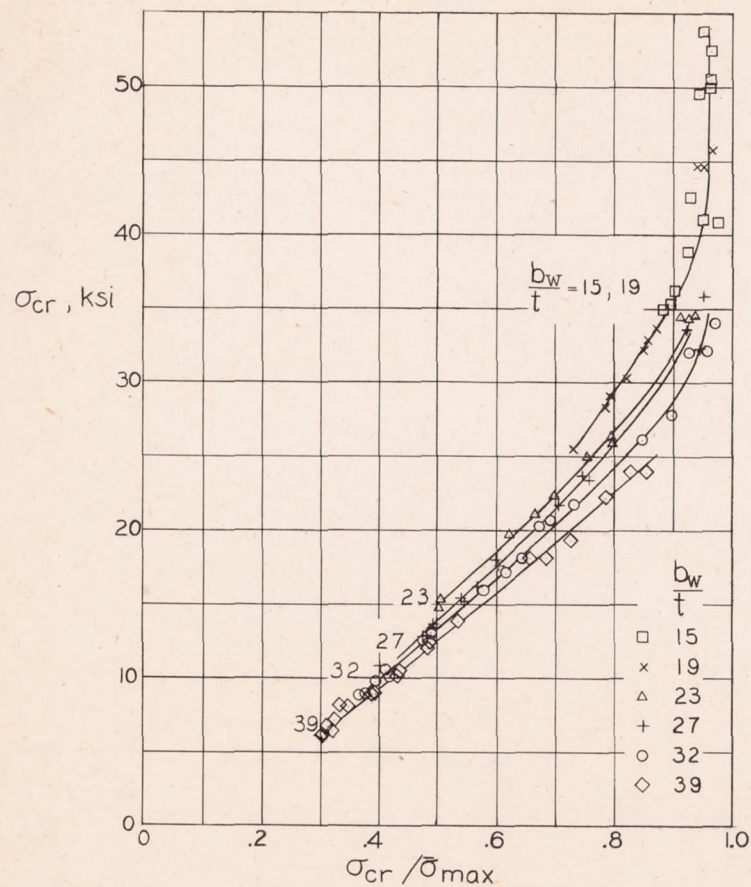
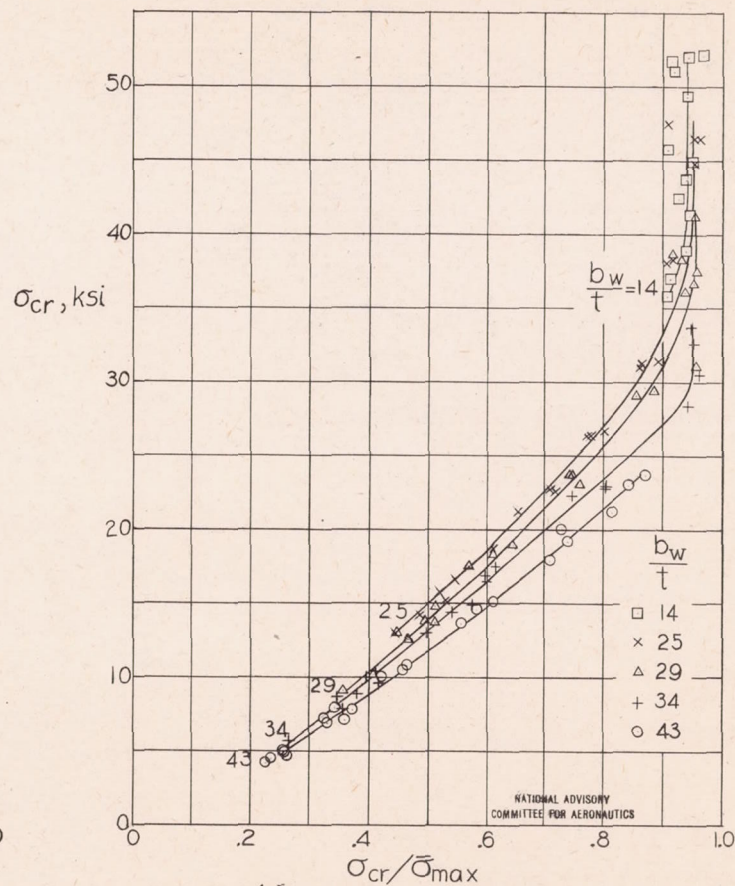


Figure 14. — Variation of σ_{cr} with σ_{cr}/η for plates of 24S-T aluminum-alloy sheet loaded in the with-grain direction, obtained from tests of formed columns; $\sigma_{cy} = 44$ ksi.

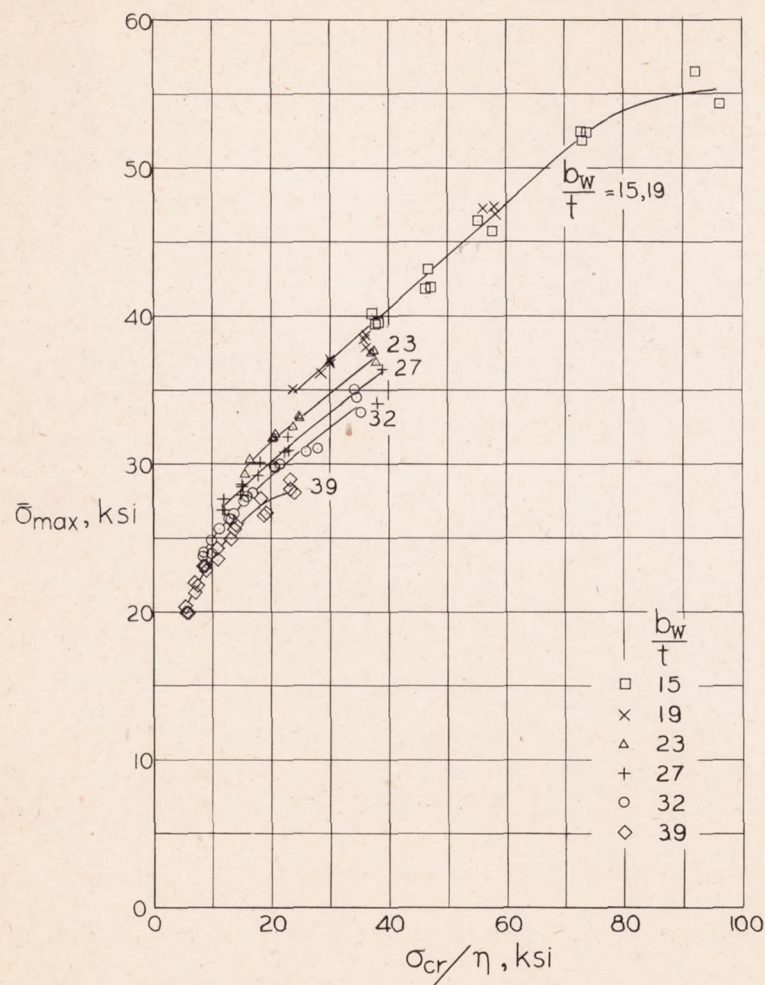


(a) Z-section.

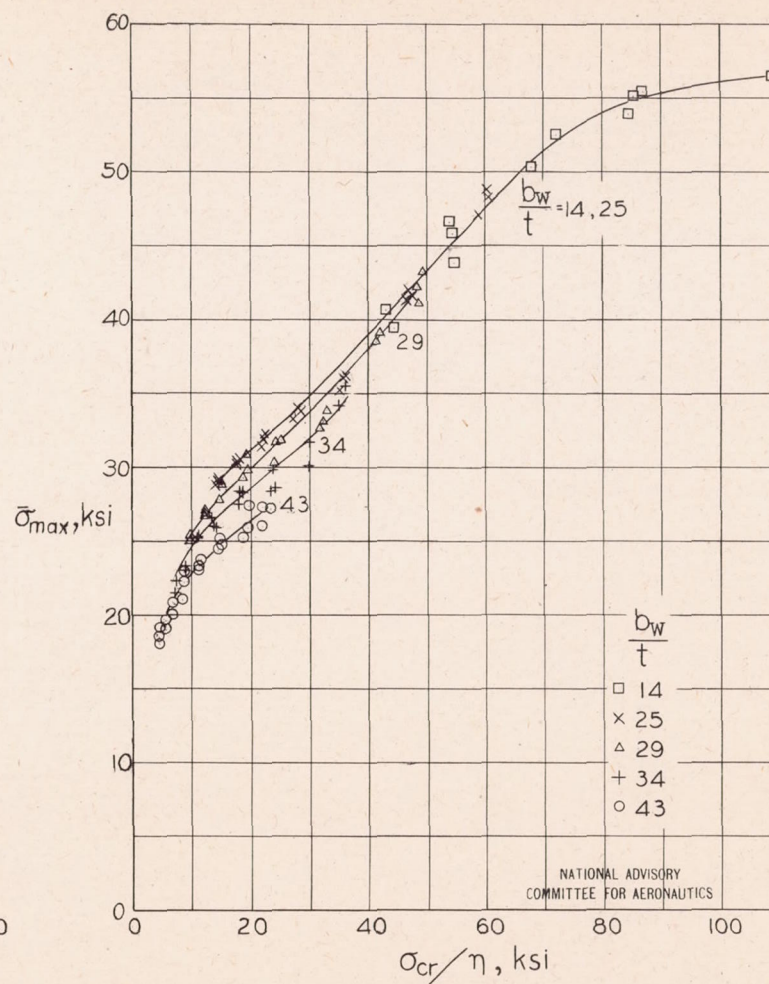


(b) Channel section.

Figure 15.- Variation of σ_{cr} with $\sigma_{cr}/\bar{\sigma}_{max}$ for formed 24 S-T aluminum-alloy columns loaded in the with-grain direction; $\sigma_{cy}=44$ ksi.

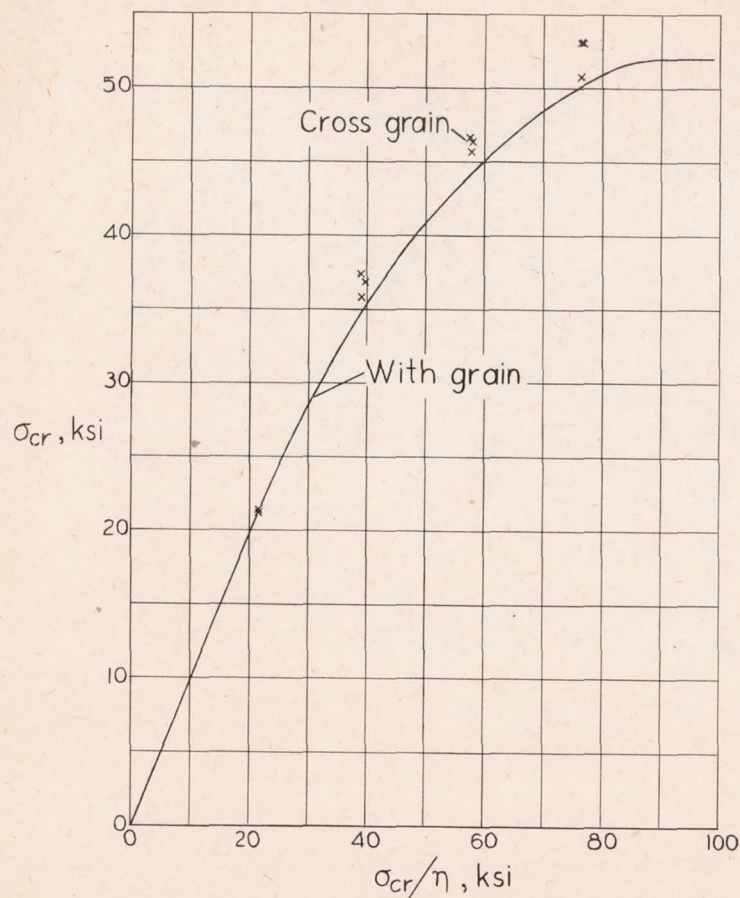


(a) Z-section.

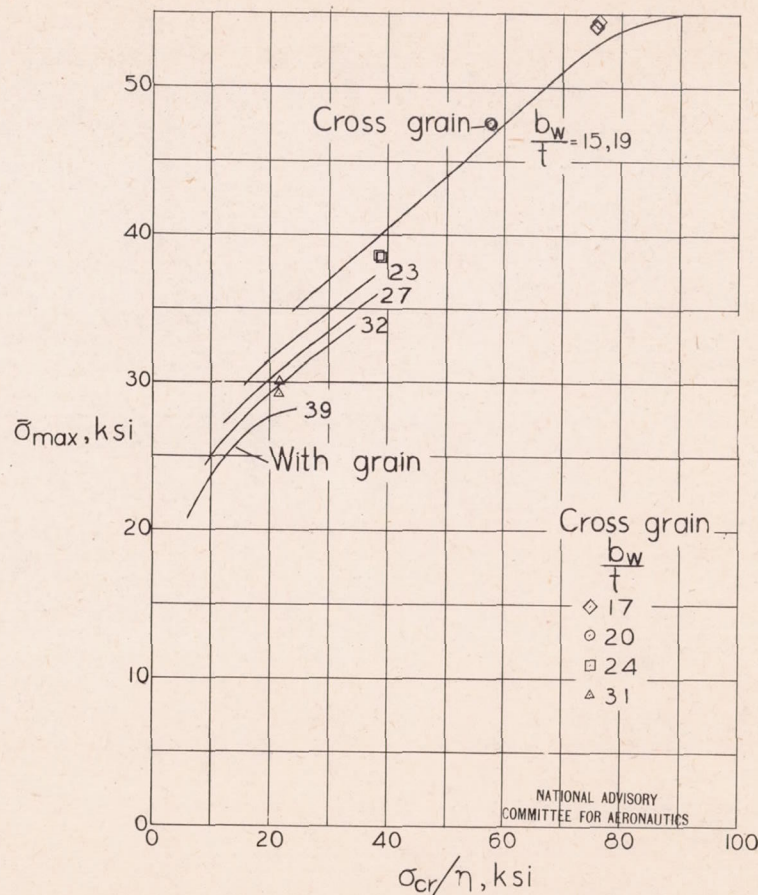


(b) Channel section.

Figure 16.-Variation of $\bar{\sigma}_{max}$ with σ_{cr}/η for formed 24S-T aluminum-alloy columns loaded in the with-grain direction; $\sigma_{cy} = 44$ ksi.



(a) Critical stress.



(b) Average stress at maximum load.

Figure 17.- Comparison of compressive strength of formed Z-section columns loaded in the with-grain and cross-grain directions. With-grain curves are taken from figures 14 and 16, and test points are for the cross-grain direction.

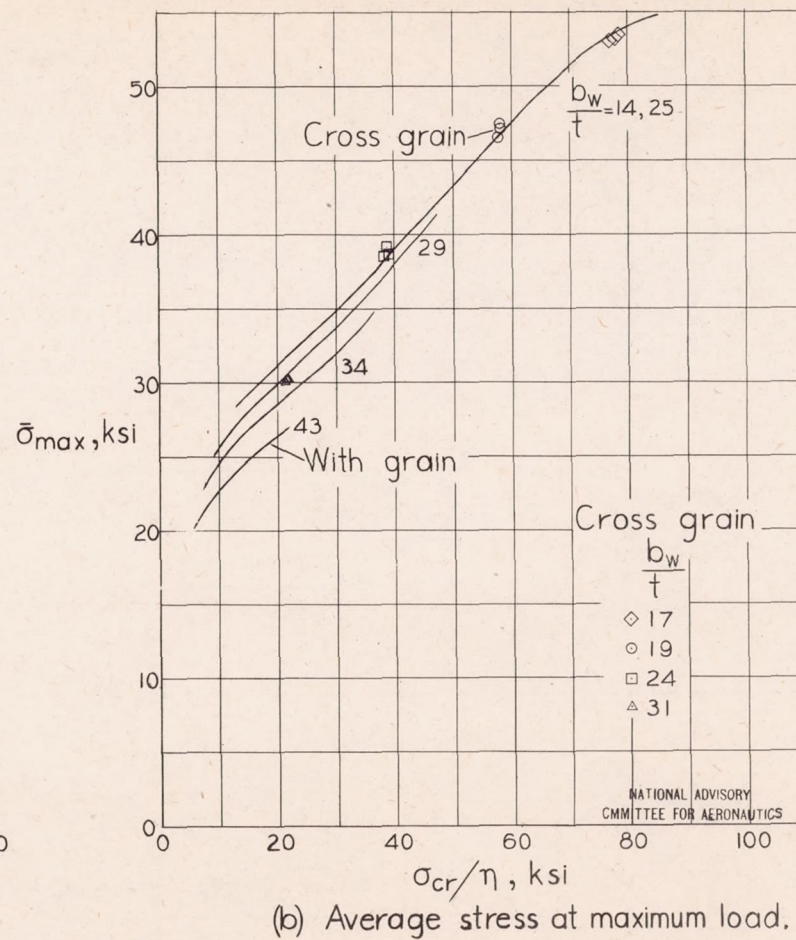
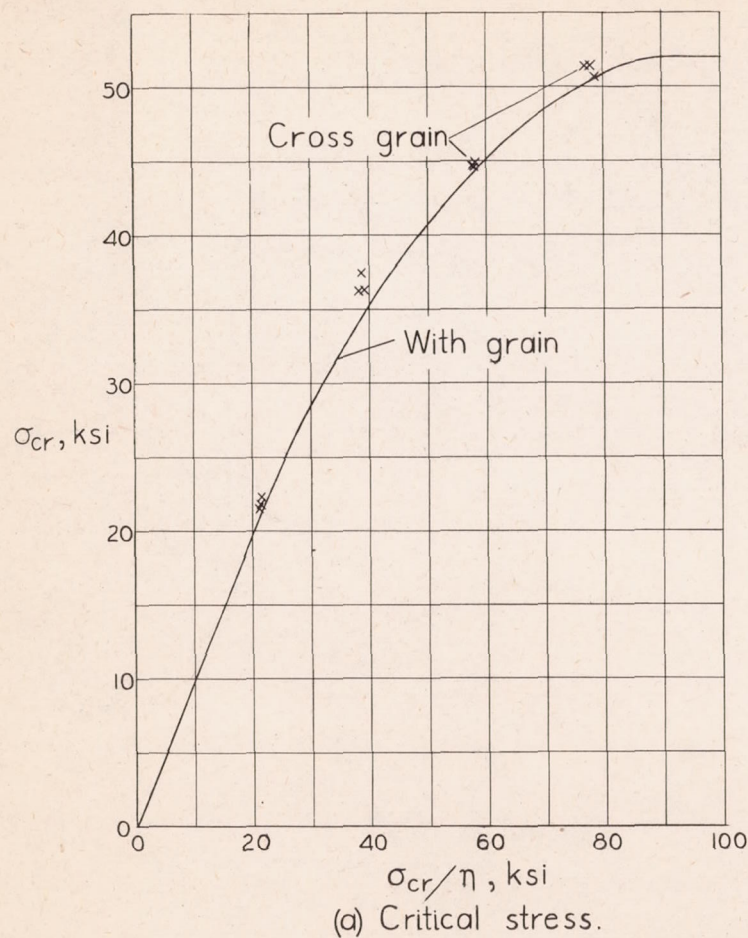


Figure 18.- Comparison of compressive strength of formed channel-section columns loaded in the with-grain and cross-grain directions. With-grain curves are taken from figures 14 and 16, and test points are for the cross-grain direction.

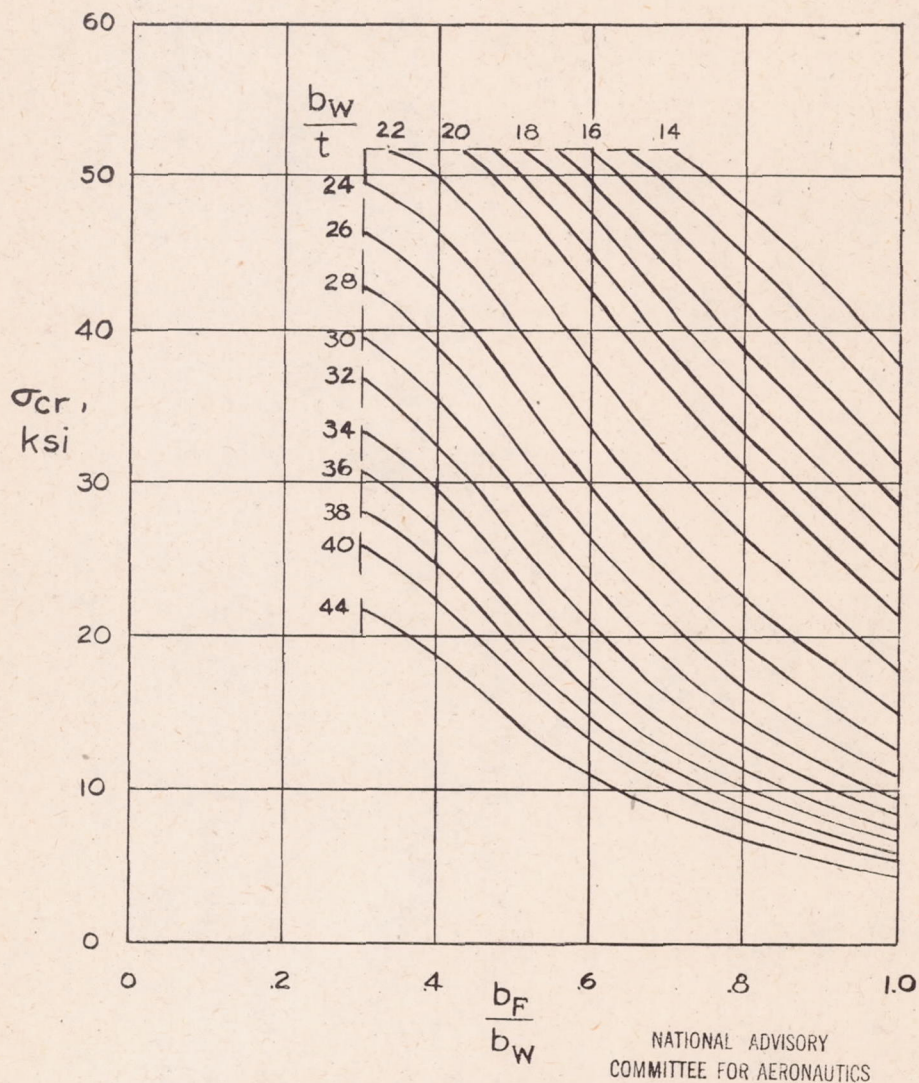


Figure 19. - Design chart for σ_{cr} for formed 24S-T aluminum-alloy Z- and channel-section columns that develop local instability loaded in the with-grain direction; $\sigma_{cy} = 44$ ksi.

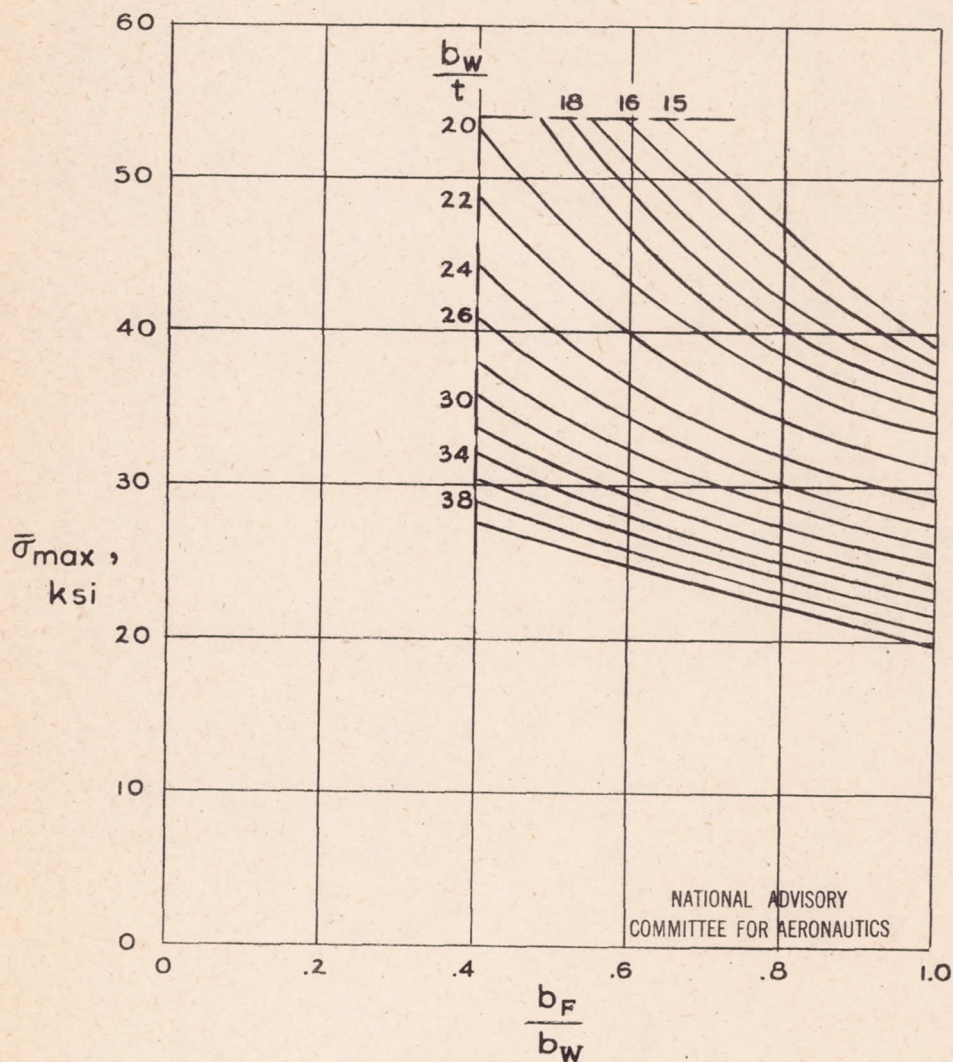


Figure 20.- Design chart for $\bar{\sigma}_{max}$ for formed 24S-T aluminum-alloy Z-section columns that develop local instability loaded in the with-grain direction; $\sigma_{cy}=44\text{ksi}$.

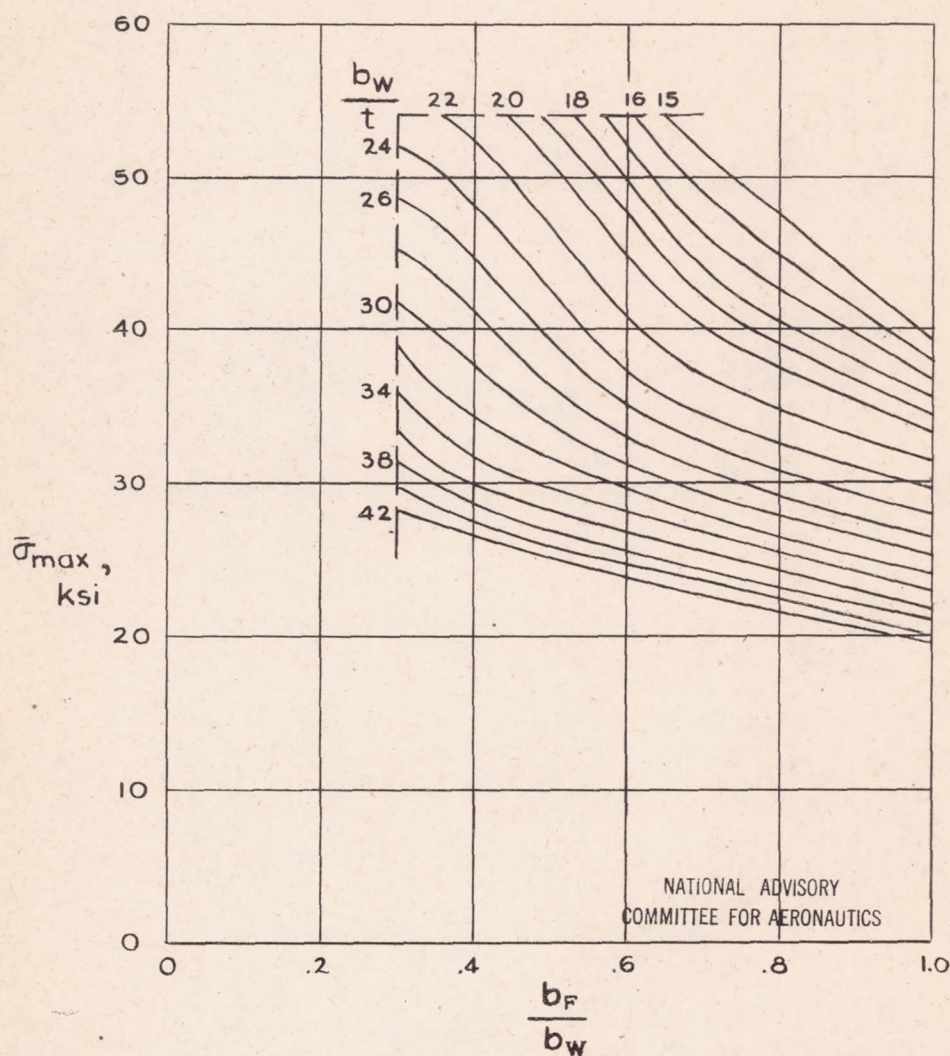


Figure 21. - Design chart for $\bar{\sigma}_{\max}$ for formed 24S-T aluminum-alloy channel-section columns that develop local instability loaded in the with-grain direction; $\sigma_{cy} = 44 \text{ ksi}$.